Comb Polymers with Triazole Linkages under Thermal and Mechanical Stress

Charlotte Petit,[ab] *Mahdi Abbasi,*[c] *Tobias Fischer,*[ab] *Manfred Wilhelm,*[*c] *Anja S. Goldmann,*[*ab] *Christopher Barner-Kowollik*[*ab]

[a]School of Chemistry, Physics and Mechanical Engineering, Queensland University of Technology (QUT), 2 George Street, Brisbane, QLD 4000, Australia. E-Mail: a.goldmann@qut.edu.au; christopher.barnerkowollik@qut.edu.au

[b]Macromolecular Architectures, Institut für Technische Chemie and Polymerchemie, Karlsruhe Institute of Technology (KIT), Engesserstr. 18, 76128 Karlsruhe, Germany. E-Mail: manfred.wilhelm@kit.edu; anja.goldmann@kit.edu; christopher.barner-kowollik@kit.edu

[c]Polymeric Materials, Institut für Technische Chemie und Polymerchemie, Karlsruhe Institute of Technology (KIT), Engesserstr. 18, 76128 Karlsruhe, Germany, manfred.wihelm@kit.edu

KEYWORDS

Comb Polymers; Thermal Stability; Polymer Stability; Copper(I)-Catalyzed Alkyne-Azide Cycloaddition (CuAAC); Nitroxide-Mediated Polymerization (NMP); Activators ReGenerated by Electron Transfer (ARGET); Atom Transfer Radical Polymerization (ATRP)

ABSTRACT

Assessing the stability of molecular bonds in polymer architectures is of critical importance for determining conditions for extrusion, molding and processing. The topological complexity of branched polymers defines their strain hardening and consequently their melt strength properties, critical parameters for their exploitation in applications. Their molecular architecture is defined by the grafting density, the chain length of the backbone as well as branches. Herein, we introduce a set of polymer combs to establish an understanding of the above parameters on the stability of the popular triazole linkage – often exploited in tethering the branches to the backbone – during thermal treatment and shearing. We exploit a combination of Reversible Deactivation Radical Polymerization (RDRP) and Copper catalyzed Alkyne-Azide Cycloaddition (CuAAC) to construct comb polymers (ranging in backbone number average molecular weight from 39.9 to 55.6 kg mol^{-1} and a branch length from 3.3 to 18 kg mol^{-1}) with statistically located branches tethered via triazole-based ligation to the backbone. These polymer combs were subsequently thermally challenged at 150 °C (or 180 °C) in an inert atmosphere as well as subjected to shearing at the same temperature. The resulting molecular cleavage processes were analyzed via size exclusion chromatography (SEC) as well as SEC coupled to high resolution-electrospray ionization mass spectrometry (SEC-HR ESI MS) to establish a mechanistic image of branch debonding when it occurs. Further, by virtue of this approach, we establish an in-depth understanding of how the comb architecture dictates its stability under otherwise unchanged chemical bonding conditions via triazole units, allowing to adopt design criteria for generating thermally and mechanically stable comb structures.

INTRODUCTION

Understanding the behavior of materials on a molecular level during the processing of polymer-based compounds is highly relevant for enhancing knowledge on their degradation mechanism and, thus, enable degradation control. Processing of polymers by extrusion and injection molding commonly requires elevated temperatures (up to 250 °C) and high pressures (up to 300 bar) that challenge and stress most polymeric materials.[1] Presence of branched structures in polymer melt and solutions controls the rheological behaviors of polymers, including shear and extensional viscosity as well as normal stresses. [2] The stress response of a plethora of polymers such as H-shaped,[3] star,[4, 5] comb[6-10], pom-pom[3] and cayley-tree [11, 12] structures has been investigated under linear and nonlinear rheology. These well-defined branched polymers have either one or two branched points per molecule (i.e. star, H-shaped and pom-pom) or multiple branched points (i.e. comb and cayley-tree), although the average distance between their branched points is longer than one entanglement. The thermomechanical stability of sparsely branched structures strongly depends on the chemical nature of junctions (e.g. ligation points) between the backbone and side chains, where the stress on the polymer segments accumulates and releases slower than the outer layers due to the higher frictions. However, increasing the grafting density on the backbone affects the average conformation of backbone and side chains due to the tight spacing between the branch points, and consequently can change the thermomechanical stability of branched polymers.

Comb polymers are based on a backbone featuring linear side chains connected via ‘grafting onto’, ‘grafting from’ or ‘grafting through’ processes.[13, 14] A ‘grafting onto’ process requires reactive entities on the backbone as well as branches. The main advantage of the ‘grafting onto’ process is the control of molecular weights and dispersities of both the backbone and the branches.[14] However, due to the potentially low concentration of functional groups and the well-defined target

structures, high yielding and regio-specific reactions are required. Click chemistry is a suitable tool to graft polymer chains since it is characterized by the absence of (or presence of only limited) side reactions, mild reaction conditions and high conversion.[15-18] Among the reactions at least partially fulfilling the stringent click criteria,[19] the copper-catalyzed azide-alkyne cycloaddition (CuAAC), described for the first time in 2001 by Sharpless and colleagues,[20] is arguably the most employed ligation.[21] The selective and orthogonal CuAAC is a catalyzed variant of the Huisgen 1,3-dipolar cycloaddition [20] affording complete regioselectivity conducive to the formation of 1,4-disubstituted-1,2,3-triazole linkages. The use of CuAAC within polymer chemistry was reported for the first time by Hawker, Sharpless, Fokin and coworkers in 2004[21] and applied – since then – for the synthesis of well-defined macromolecular architectures.[18, 22-24] To design such structures, reversible-deactivation radical polymerization (RDRP) may be used to form building blocks prior to the ligation reaction. The RDRP techniques, including reversible addition fragmentation chain transfer polymerization (RAFT),[25, 26] atom transfer radical polymerization (ATRP)[27-30] and nitroxide-mediated polymerization (NMP)[31, 32] are powerful tools for building polymers with controlled molecular weight, dispersity and chain-end functionalities.[33-36] For instance, the fusion of ATRP and CuAAC has been exploited by Matyjaszewski and colleagues for the preparation of well-defined star-like structures based on a polystyrene core and poly(ethylene oxide) arms,[37] by Turro and team who synthetized photocleavable linear and star-like macromonomers,[38] by Haddleton and coworkers for the synthesis of sequence defined PMMA-based macromolecules[39] or by Yagci and colleagues who prepared comb polystyrene via a 'grafting from' process.[40] In our current study, we employ NMP to synthetize the backbone, ATRP for the synthesis of the branches and CuAAC to form the comb polymers.

In an earlier effort to establish a fundamental understanding of the stability of ligation points in strictly linear macromolecular architectures, we reported linear polymers containing a triazole moiety in the middle of the chain, an ester group randomly placed in the polymer chain and/or a bromine atom as an end chain, and studied their stability under thermal and thermomechanical stress in an inert atmosphere.[41] A complete molecular analysis revealed that in the absence of a bromine atom as an end chain, both the ester groups and the triazole moiety are stable during thermal treatment (at 180 °C). Therefore, in order to avoid any side reactions occurring due to the elimination of the protonated halogen (e.g. HBr), the terminal Br atom has to be carefully removed after ATRP and prior thermal treatment, including in the current study. In addition, in a recent study, Yan *et al.* reported that the incorporation of amide groups in polymers effectively increase the thermal stability of the resulting polymers.[42] Since the triazole linkage point is stable under conditions close to the ones of extrusion or molding (high temperature and pressure i.e. up to 250°C and 300 bar) when located in linear polymers,[43] it is a critical next step to understand their stability when placed into more complex architectures such as comb polymers. Their unique physical and chemical properties as well as their wide range of potential applications (e.g. thermoforming, compression and transfer molding, extrusion, injection molding) are of critical importance for both the academic and industrial communities.[6] To the best of our knowledge, there exists no understanding regarding the thermomechanical stability of the triazole moiety in branched structures or more particularly, in comb-branched topologies.

Thus, the present study seeks to establish the stability of triazole linkage points towards temperature and shearing when embedded in comb topologies. We investigate the stability of triazole linkages in polymer combs prepared via a combination of radical polymerization processes (NMP and ARGET ATRP) and CuAAC (**Scheme 1**) with a varied number of triazole linkages

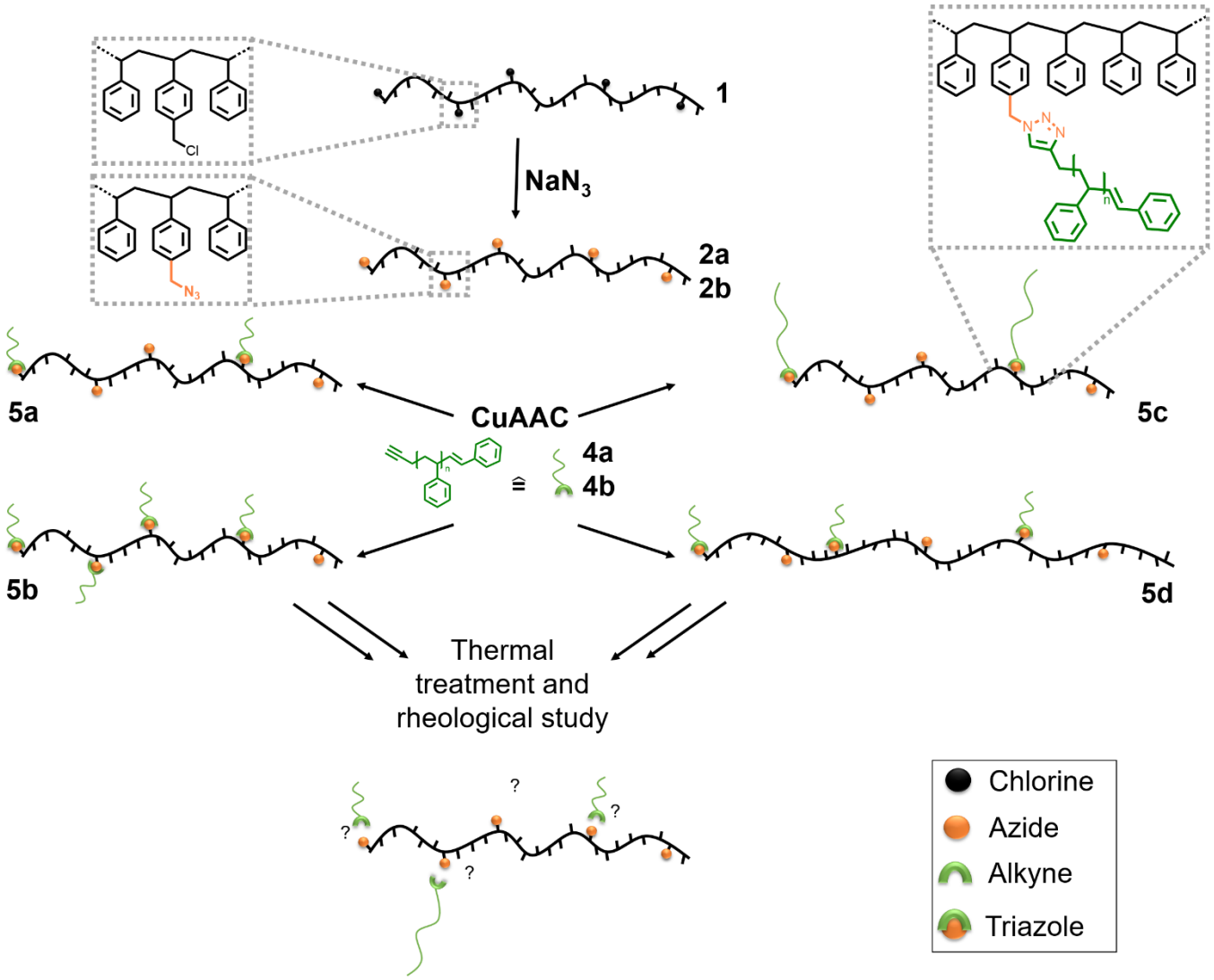

Scheme 1. Overview of the preparation and stability study of polystyrene-based combs. Preparation of poly(styrene-*stat*-chloromethylstyrene) (PS-*stat*-PCMS) **(1)** as well as poly(styrene-*stat*-azidemethylstyrene) P(S-*stat*-azideMS) backbones **(2a-b),** alkyne functionalized side chains **(4a-b)** and the resulting polymer combs **(5a-5d)**.

(1 to 10% grafting) and varied chain length for both backbones (39.9 and 55.6 kg mol^{-1}) and branches (3.3 and 18.1 kg mol^{-1}). We thus aim to assess the processability of the synthetized combs under elevated temperature and shearing conditions, underpinned by an in-depth thermal and thermomechanical mechanistic stability assay.

EXPERIMENTAL SECTION

Synthesis of Alkyne-containing Backbones

Styrene (**2a**: 11.8 mL, 104 mmol, 750 equiv.; **2b**: 6 mL, 52 mmol, 750 equiv.), 4-(chloromethyl)styrene (**2a**: 0.58 mL, 4.13 mmol, 30 equiv.; **2b**: 0.58 mL, 4.13 mmol, 60 equiv.) and TEMPO initiator (**2a**: 36 mg, 0.14 mmol, 1.0 equiv.; **2b**: 18 mg, 0.07 mmol, 1.0 equiv.) was dissolved in (8 mL for **2a** and 4 mL for **2b**) dry toluene in a flame-dried Schlenk flask and deoxygenated by four consecutive freeze–pump–thaw cycles. Subsequently, the reaction mixture was placed into an oil bath tempered at 125 °C. After 20 (**2a**) or 48 h (**2b**), the polymerization was stopped by cooling the flask with liquid nitrogen and opening it to the atmosphere. The crude product was diluted with THF (20 mL) and precipitated twice into cold methanol (200 mL). The polymer was afforded as a white powder (4.2 g, 0.10 mmol (**2a**); 3.6 g, 0.06 mmol (**2b**)) by filtration and dried under high vacuum. The dried polymer was diluted in DMF with NaN_3 (4.13 mmol, 60 equiv.) and stirred at ambient temperature overnight. Afterwards 100 mL of ethyl acetate was added and the sodium azide was extracted two times with distilled water. The organic phase was dried under magnesium sulfate and reduced under high vacuum. The residue was diluted with THF (20 mL) and precipitated twice into cold methanol (200 mL). The polymer was afforded as white powder (4.0 g, 0.10 mmol (**2a**); 3.3 g, 0.06 mmol (**2b**)) by filtration and dried under high vacuum. ^{1}H NMR (400 MHz, $CDCl_3$, δ): 7.26–6.20 (m, aromatic protons of PS), 2.50–0.84 (m, aliphatic protons of PS). **2a**: M_w=39.9 kg·mol^{-1}, $Đ$ = 1.14, $\%_{azide}$ = 12 mol%; **2b**: M_w=55.6 kg·mol^{-1}, $Đ$ = 1.25, $\%_{azide}$ = 8 mol%.

Synthesis of the Azide-terminal Side Chains

The side chains were prepared via ARGET ATRP in anisole (1 mL) at 90 °C using styrene (25 mL, 0.2 mol) as monomer, $CuBr_2$ (14 mg, 64.9 mmol) as catalyst, Me_6TREN (6 µL, 22.4 mmol) as reductive agent and $Sn(EH)_2$ (45 µL, 0.14 mmol) as ligand. The polymerization was initiated by TMS-protected propargyl bromine (0.14 mmol) and the protecting group was removed using TBAF (10 eq.) in THF at room temperature overnight prior the following click reaction. The residue was diluted with THF (20 mL) and precipitated twice into cold methanol (200 mL). The polymer was afforded as a white powder (**4a**: 100 mg; 1.0 mmol; **4b**: 150 mg, 1.5 mmol) by filtration and dried under high vacuum.

Synthesis of the Comb polymers via CuAAC

The backbone **2** (3 mmol; 2a: 120mg, 2b: 167 mg), side chains **4** (equivalents according to the targeted degree of grafting), $Cu(II)SO_4 \cdot 5 \cdot H_2O$ (0.25 g, 1 mmol) and sodium ascorbate (0.2 g, 1 mmol) were dissolved in 10 mL DMF. After stirring at ambient temperature overnight, azide-functionalized resin[44] was added (ratio resin:side chains is of 1:1) as well as $Cu(II)SO_4 \cdot 5 \cdot H_2O$ (0.25 g, 1 mmol) and sodium ascorbate (0.2 g, 1 mmol) in order to react with the excess of side chains and was stirred again overnight at ambient temperature. The free alkyne-functionalized branches react thus with the azide-functionalized resin. After filtering off the insoluble resin, 200 mL of ethyl acetate was added to the reaction mixture and was extracted twice in 50 mL of EDTA (5 wt%) solution to remove the copper. The organic phase was dried over Na_2SO_4 and the solvent was removed under reduced pressure. The purified polymer was obtained by two-fold precipitation into cold methanol. The precipitate was filtered off and dried under high vacuum to afford the comb polymer as a white powder (**5a**: 100 mg, 1.7 µmol ; **5b**: 120 mg, 0.68 µmol; **5c**: 90 mg, 0.79 µmol; **5d**: 110 mg, 1.1 µmol).

Rheometry - Sample preparation

As the investigated samples are temperature sensitive, the samples need to be carefully press molded at relatively low temperature and short heating time (120°C for 5 min) before rheological measurements. The samples were placed between 13 mm Teflon disks in a hot press, where vacuum was applied and heated to 120 °C. After 5 min, pressure was applied in order to restrain the sample between the Teflon disks and to remove any trapped air. The heating was turned off and the samples were removed from the press at ambient temperature. The rheological characterization was carried out under nitrogen atmosphere using ARES-G2 rheometer, TA Instruments. The small amplitude oscillatory shear (SAOS) measurements in the mode of dynamic time sweep test were conducted using parallel plate geometry (13 mm, gap ≈ 1 mm) under strain amplitude of γ_0 = 0.25 and a frequency of 0.05 Hz at 150 °C and 180 °C.

RESULTS AND DISCUSSION

In the following, we detail the generation of the building blocks prior to a theoretical assessment dictating the topology choice of synthetized branched polymers.

Synthesis of the Building Blocks

In order to determine the rheological properties of a material, we have to consider the role of physical entanglements. Entanglements and topology control the melt viscosity in shear and elongation of the constitutive polymer. An entanglement is defined as an interlace of chains leading to the formation of a (non-) permanent junction within a polymer material.[45] Below the molecular weight of an entanglement, M_e, the polymer chains behave like a Rouse chain and zero shear viscosity, $\eta_{0,}$ increases linearly with molecular weight, $\eta_0 \propto M$. Above 2-3 times M_e, the zero shear viscosity, for a linear topology, increases strongly via a cubic scaling law, $\eta_0 \propto M^3$, providing thus longer relaxation time under shear deformations as $\eta_0 \propto \tau$. For example, the M_e of polystyrene is close to15 kDa. Below M_e, PS is a brittle polymer whereas 2-3 times above M_e, PS can be molded and exhibits melt strength. In our study, we targeted backbones with molecular weights exceeding 2 to 3 times M_e in order to ensure the backbones feature significant viscosity prior to grafting. The poly(styrene-*stat*-chloromethylstyrene) (PS-stat-PCMS) backbones, synthetized via NMP, were modified to substitute the methyl chlorine groups by methyl azide groups **(Scheme 1** and **Scheme 2)**.

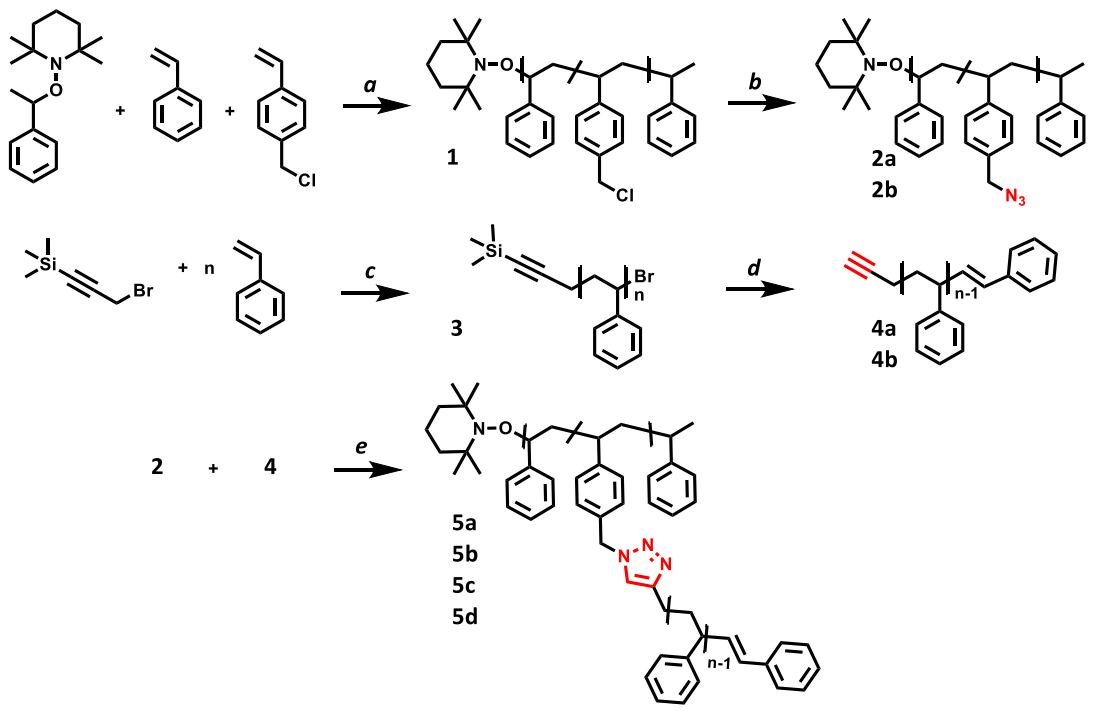

Scheme 2. Synthetic strategy for the preparation of poly(styrene-*stat*-chloromethylstyrene) (PS-*stat*-PCMS) **(1)** as well as poly(styrene-*stat*-azidemethylstyrene) P(S-*stat*-azideMS) backbones **(2)** (**2a**: M_w=39.9 kg·mol^{-1}, $Đ$ = 1.14, $\%_{azide}$ = 12 mol%; **2b**: M_w=55.6 kg·mol^{-1}, $Đ$ = 1.25, $\%_{azide}$ = 8 mol%) alkyne functionalized side chains **(4)** (**4a**: M_w=3.3 kg·mol^{-1}, $Đ$ = 1.05; **4b**: M_w=18.1 kg·mol^{-1}, $Đ$ = 1.08) and the resulting polymer combs **(5)** (details given in **Table 1**). ***a***: NMP, 125 °C; ***b***: NaN_3, DMF, a.t., 12h; ***c***: $CuBr_2$, Me_6TREN, $Sn(EH)_2$, anisole, 90 °C; ***d***: TBAF, THF, a.t., 16h; ***e*** $Cu(II)SO_4$, sodium ascorbate, DMF, a.t., 16h.

After post-polymerization modification of the backbones (from poly(styrene-*stat*-chloromethylstyrene) (PS-*stat*-PCMS) to poly(styrene-*stat*-azidemethylstyrene) P(S-*stat*-azideMS)), ^{1}H-NMR analysis using the resonance of the protons associated with the CH_2 group in α-position of the azide function at 4.2 ppm **(Figure S1 and 3)**, allowed for the quantification of the azide functions (x_{NMR}) in the backbones **2a** and **2b** at 8 and 12 mol%, respectively. The total number of azide-functionalizedrepeating units is calculated following the equation **(1)**.

$$\text{number of functionalized repeating units} = \frac{\mathrm{M_{w\ backbone}}}{\overline{\mathrm{M}_{\mathrm{unit}}}} . x_{NMR} \qquad (1)$$

with $\overline{M_{unit}}$ the number average molecular weight of one repeating unit ($x_{NMR} M_{N_3 MethylStyrene} + (1 - x)\, M_{Styrene}$ with x_{NMR} the fraction of azide functions in the backbones obtained via ^{1}H NMR and $M_{N_3 MethylStyrene}$ the molecular weight of a azide methylstyrene unit).

The number of azide-functionalized repeating units of **2a** and **2b** is 43 and 41, respectively. The molecular weight of the backbones **2a** and **2b** before and after post-polymerization modification is identical and was monitored via SEC analysis **(Figure 1)**. The side chains – synthetized via ARGET ATRP – exhibit protected alkyne end-chains **3 (Scheme 2)**. After deprotection of the branches **3** initiated with protected propargyl bromine, the resulting polymers **4a** and **4b** were analyzed via SEC **(Figure 1, S5 and S8)** exhibiting molecular weights of 3.3 and 18 kg·mol^{-1} and a monomodal distribution ($1.05 < Đ < 1.08$) suggesting a well-controlled polymerization process. The molecular structure of the end groups attached to the PS-based side chains (**4a** and **4b**) was assessed via ^{1}H-NMR (**Figure S6 and S9**) and SEC-HR ESI MS measurements in which the elimination of HBr is observed by the formation of an alkene function at the chain terminus **(Figure S7)**. In addition, the unprotected alkyne function on the polymer chain end remains intact **(Figure S7)**. Copper-catalyzed azide-alkyne cycloaddition (CuAAC) reactions subsequently fused one of the polymers **2** (**2a** or **2b**) and one of the side chains **4** (**4a** or **4b**) in different ratios, generating a library of comb polymers having grafted side chains statistically located along the backbone. The degrees of grafting are obtained by adjusting the stoichiometry according to the targeted values. Considering CuAAC as a reaction with full conversion, the degree of grafting can be tuned from the reacting mixture accordingly.

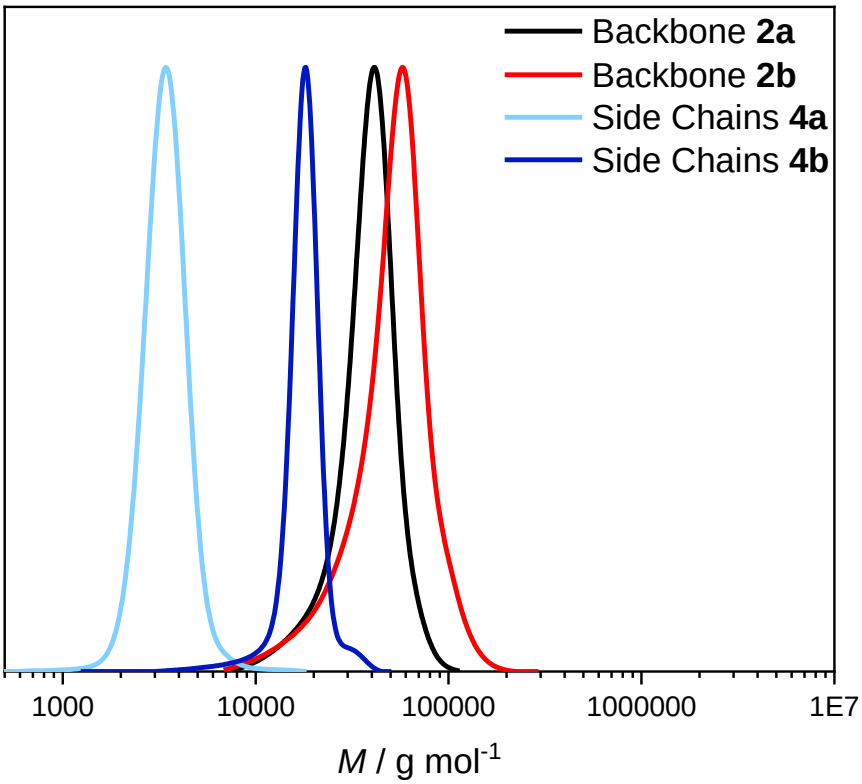

Figure 1. SEC trace of the backbones **2a** and **2b** and of the side chains **4a** and **4b** (in THF and with RI detector calibrated using linear poly(styrene) standards ranging from 476 to 2.5 × 10^6 g·mol^{-1}).

Conformation of Comb and Bottlebrush Polystyrenes in the Melt State

Branched polymers, especially comb topologies, are of significant interest due to the potential effect of the branches on the processing and rheological behaviors as well as on the mechanical properties of polymer. The conformation of the backbone and side chains in a comb architecture in the melt state is affected by the number of branches per backbone, N_{br}, the molecular weight of branches, M_{br}, and the molecular weight of backbone, M_{bb}. These three independent parameters of a comb polymer can be reduced to two parameters, M_{br} and the average molecular weight between two neighboring branch points $M_s = M_{bb}/(N_{br} +1)$. Based on scaling analyses and molecular dynamic simulation, four different conformational regimes are distinguished for comb architectures:[46, 47] **L**oosely and **D**ensely-grafted **C**omb (denoted LC and DC herein, respectively), and **L**oosely and **D**ensely-grafted **B**ottlebrushes (denoted LB and DB herein, respectively). In a LC topology, M_{br} is smaller than M_s, i.e. $M_{br} < M_s$, therefore both side chains and backbone have a random Gaussian conformation in the melt state (**Scheme 3.** Schematic representation of the pervaded volume (grey circle) in the polymer combs **5a** to **5d** with the backbones displayed in black and the branches in green (refer to Table 1 for more details about the combs)**-5a**). A further increase of the number of branches on a certain backbone, where $M_s < M_{br}$, initially results in a DC, where the pervaded volume (volume occupied by a chain which is equal to the cube of the root-mean-square end-to-end distance of a chain, $V_p = <R^2>^{3/2}$. This volume is roughly 20.8±0.8 times larger than the physical volume of the same chain [48, 49]) (**Scheme 3.** Schematic representation of the pervaded volume (grey circle) in the polymer combs **5a** to **5d** with the backbones displayed in black and the branches in green (refer to Table 1 for more details about the combs)**-5b**) of each side chain comprises many side chains from the same comb. Therefore, the interpenetration of side chains from the adjacent combs is reduced.

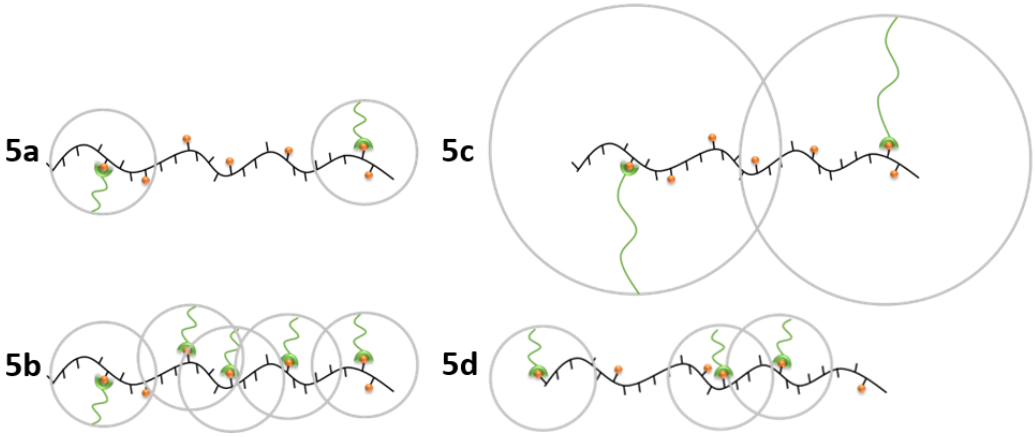

Scheme 3. Schematic representation of the pervaded volume (grey circle) in the polymer combs **5a** to **5d** with the backbones displayed in black and the branches in green (refer to Table 1 for more details about the combs)

A further increase of branches or a reduction of the M_s results in a loosely grafted bottlebrush (LB) topology, where the side chains of neighboring molecules cannot interpenetrate other side chains. Under such conditions, the backbone of an LB molecule undergoes an extension to form a more stretched conformation rather than an unperturbed random Gaussian conformation, due to the tight spacing between the branching points. However, in this regime, the side chains are still unperturbed. In a densely grafted bottlebrush, DB, the backbone is already fully stretched and side chains undergo extension. A densely grafted bottlebrush has a fully segregated structure. Equations 2 to 5 represent the criteria for these four conformations based on the number of entanglements in a backbone, $Z_{bb} = M_{bb}/M_e$, number of entanglements in side chains, $Z_{br} = M_{br}/M_e$, and number of entanglements in a branch point spacing[50], $Z_s = M_s/M_e$:

$$Z_{br} < Z_s \quad \text{Loosely-grafted combs, LC} \quad (2)$$

$$\frac{(Z_{br}M_0/M_e)^{\frac{1}{2}}\nu}{(bl)^{\frac{3}{2}}} < Z_s < Z_{br} \quad \text{Densely-grafted combs, DC} \quad (3)$$

$$\frac{\nu M_0}{M_e bl^2} < Z_s < (Z_{br}M_0/M_e)^{1/2}\nu/(bl)^{3/2} \quad \text{Loosely-grafted bottlebrushes, LB} \quad (4)$$

$$M_0/M_e < Z_s < \nu M_0/(M_e bl^2) \quad \text{Densely-grafted bottlebrushes, DB} \quad (5)$$

M_0 and M_e are the monomeric molecular weight and entanglement molecular weight of a linear polymer, respectively. The molecular parameters ν, l and b are monomeric volume, monomeric length, and Kuhn length (related to the stiffness of the polymer chains), respectively. According to equations 2 to 5 and using styrene as the monomer with M_0 = 104.15 g·mol^{-1}, M_e = 14,500 g·mol^{-1}, ρ = 0.909 g cm^{-3}, monomeric volume ν = 0.19 nm^3, Kuhn length b = 1.8 nm, C_∞ = 9.5 and the monomeric length $l = b / C_\infty$ = 0.19 nm, equations 6 to 9 are valid for comb and bottlebrush polystyrenes:

$$M_{br} < M_s \quad \text{Loosely-grafted comb-PS, LC-PS} \quad (6)$$

$$9.7M_{br}^{0.5} < M_s < M_{br} \quad \text{Densely-grafted comb-PS, DC-PS} \quad (7)$$

$$304.5 < M_s < 9.7M_{br}^{0.5} \quad \text{Loosely-grafted bottlebrush-PS, LB-PS} \quad (8)$$

$$104.15 < M_s < 304.5 \quad \text{Densely-grafted bottlebrush-PS, DB-PS} \quad (9)$$

Synthesis of the Combs

The azide functions in the backbone **2a** (M_w=39.9 kg·mol^{-1}, $Đ$ = 1.14, %$_{azide}$ = 12 mol%) were ligated via CuAAC with the alkyne end chains of the branches **4a** (M_w=3.3 kg·mol^{-1}, $Đ$ = 1.07) or **4b** (M_w=18.1 kg·mol^{-1}, $Đ$ = 1.08) with different number of branches per backbone (**Figure 2** and

Table 1) to afford three comb polymers with various grafting densities (from 1 to 10 %), length of backbone and side chains, **5a** (M_w=57.7 kg·mol^{-1}, $Đ$ = 1.20), **5b** (M_w=175.7 kg·mol^{-1}, $Đ$ = 1.43) and **5c** (M_w=113.4 kg·mol^{-1}, $Đ$ = 1.27). The N_3 functions in the backbone **2b** (M_w=55.6 kg·mol^{-1}, $Đ$ = 1.25, $\%_{azide}$ = 8 mol%) were coupled with the alkyne functions of **4a** (M_w=3.3 kg·mo^{-1}, $Đ$ = 1.05) to afford the comb **5d** (M_w=97.5 kg·mol^{-1}, $Đ$ = 1.25) (**Figure 2** and **Table 1).**

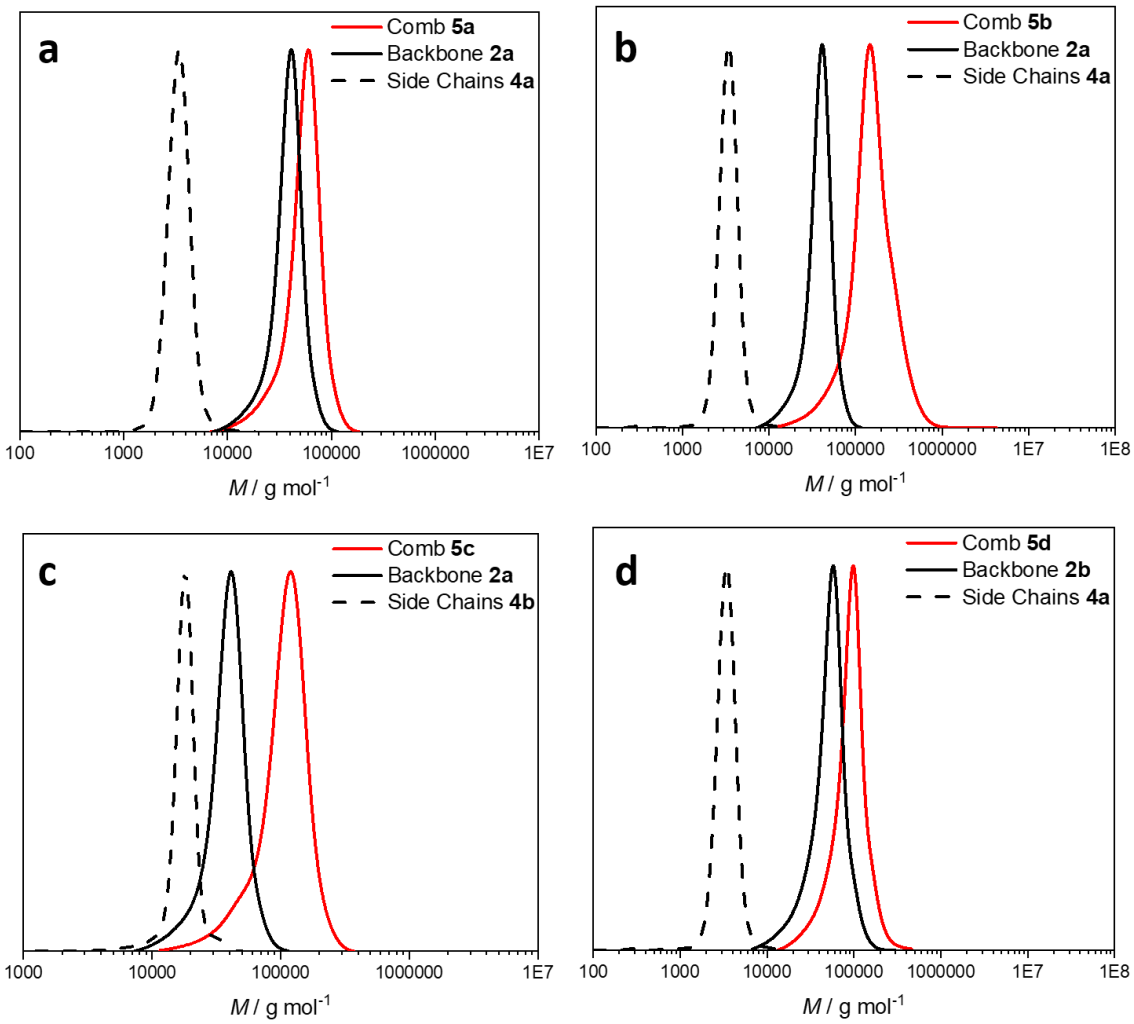

Figure 2. SEC traces of the combs **5a** (M_w=57.7 kg·mol^{-1}, $Đ$ = 1.20) (**a**), **5b** (M_w=175.7 kg·mol^{-1}, $Đ$ = 1.43) (**b**), **5c** (M_w=113.4 kg·mol^{-1}, $Đ$ = 1.27) (**c**) and **5d** (M_w=97.5 kg·mol^{-1}, $Đ$ = 1.25) (**d**) after CuAAc with the backbones **2a** (M_w=39.9 kg·mol^{-1}, $Đ$ = 1.14, $\%_{azide}$ = 12 mol%) (**a-c**), **2b** (M_w=55.6 kg·mol^{-1}, $Đ$ = 1.25, $\%_{azide}$ = 8 mol%) (**d**) and the side chains **4a** (M_w=3.3 kg·mol^{-1},

$Đ$ = 1.07) (**a**, **b** and **d**), **4b** (M_w=18.1 kg·mol^{-1}, $Đ$ = 1.08) (**c**) (in THF with MALLS detection for the comb polymers and RI calibrated with linear PS samples for the linear polymers).

Equations 6 to 9 were employed to distinguish the topologies of the comb structures synthesized in **Table 1**. The calculation of the M_s values of the samples **5** reveals that the combs **5a**, **5c** and **5d** are loosely branched (LC), while the comb **5b** is densely branched (DC) (**Table 1**).

Due to the complex conformation of comb polymers, the use of SEC coupled to a light scattering detector is required to obtain their absolute molar masses. Thus, the comb polymers were analyzed via SEC coupled with a Multiple Angle Laser Light Scattering (MALLS) detector and the resulting traces of the comb polymers are depicted in

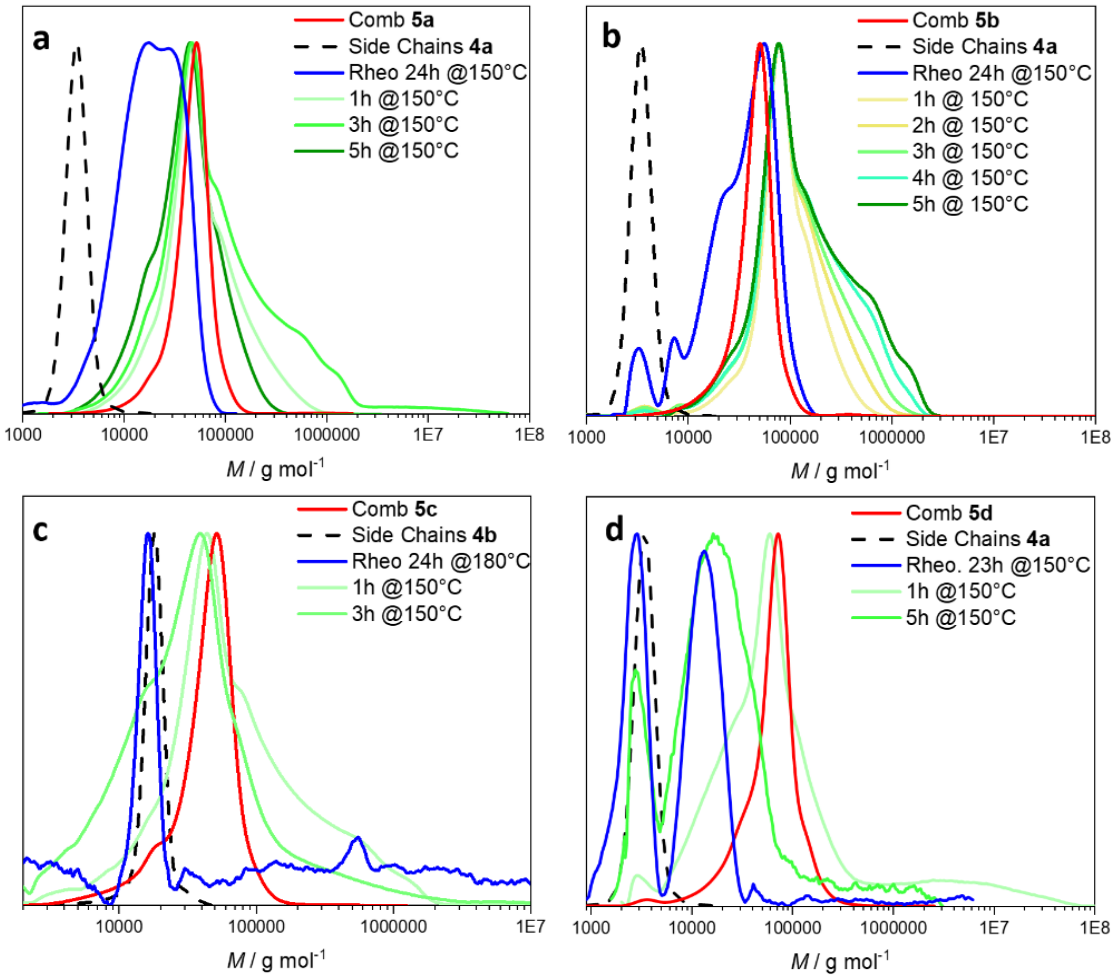

Figure 4. In addition, the linear regression calculated for the MALLS detection (**Figures S11, 14, 17, 20**) confirms the accuracy of the calculated weight average molecular weight. The characteristics of the resulting comb polymers are detailed in **Table 1**, in which the number of grafted polymer units is calculated using the weight average molecular weight obtained from SEC-MALLS measurements following **Equation 2**. For the linear polymers, the weight average molecular weight was calculated from refractive index detection since their topology (linear) allows an accurate linear calibration with linear PS standards.

$$N_{br} = \frac{M_{w\ comb} - M_{w\ backbone}}{M_{w\ side\ chain}} \qquad (10)$$

The percentage of grafting ($mol\%_{grafting}$) in **Table 1** represents the ratio between the number of grafted polymer units (i.e. number of branches) (**Equation 10**) and the total number of functionalized polymer units (**Equation 1**). The percentage of grafted polymer units determined via ^{1}H-NMR in **Table 1** is based on the resonances between 4.0-4.5 ppm and between 5.0-5.5 ppm corresponding to the free azide functions and the grafted ones respectively and is detailed in the **Equation S1**.

The SEC traces of the synthetized comb polymers from **5a** to **5d** are depicted in **Figure 2** and reveal monomodal distributions demonstrating the homogeneous grafting of the backbones.

Table 1. Description and characterization data of the comb polymers generated via CuAAC from backbones **2a** and **2b** and the side chains **4a-4b**. [a]The labeling of the samples are defined as followed: Polymer type-$M_{w(backbone)}$-Number of branches-$M_{w(branches)}$. [b]Refer to **Figure 3**.

Entry	[a]Sample	Backbone	Side chains	[b]N_{br}	[b]M_s	% grafted units^{NMR}	% grafted units^{SEC}	$M_{n\ MALLS}$	$Đ$	[b]Topology
5a	PS-40k-5-3.3k	**2a**	**4a**	5	6700	2.1	1.2	57 700	1.20	LC
5b	PS-40k-39-3.3k	**2a**	**4a**	39	1000	8.5	10.1	175 700	1.43	DC
5c	PS-40k-4-18k	**2a**	**4b**	4	8000	1.2	1.0	113 400	1.27	DC
5d	PS-55k-12-3.3k	**2b**	**4a**	12	4300	3.4	2.3	97 500	1.25	LC

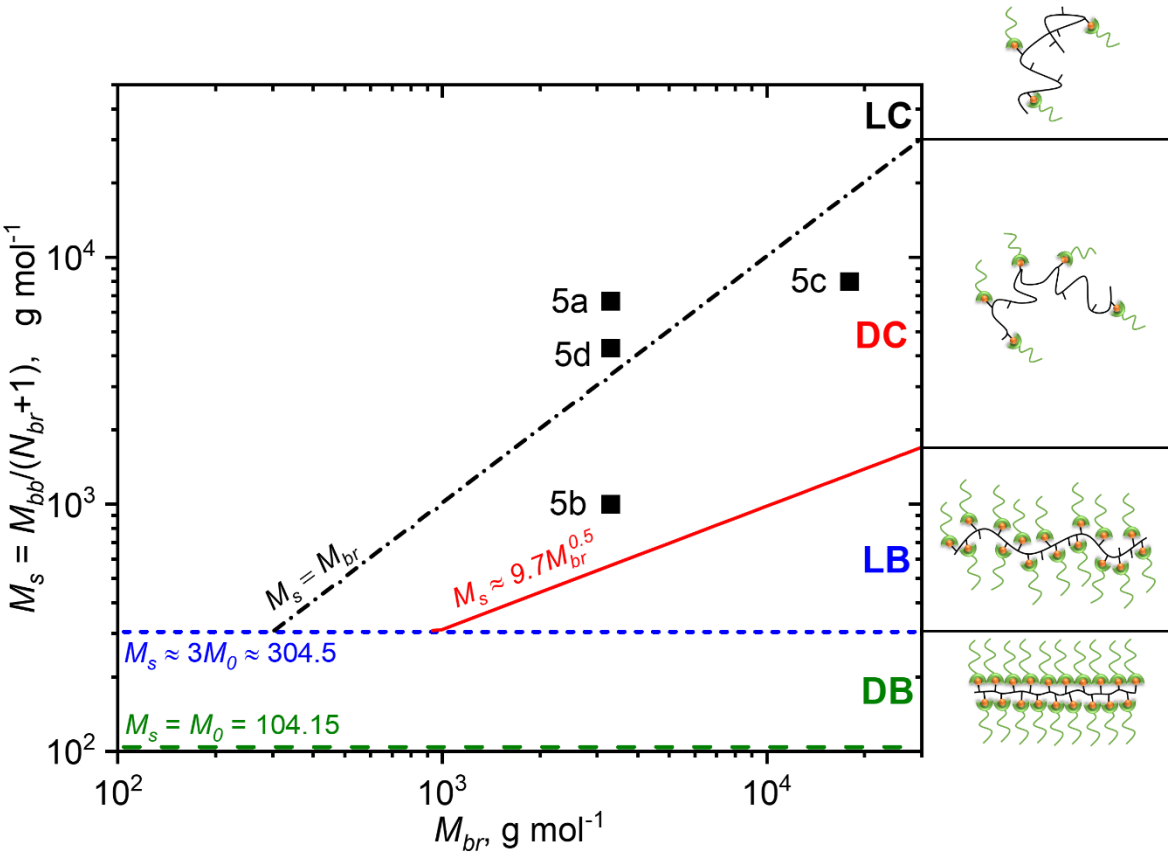

Figure 3. Four conformation regimes of comb and bottlebrush polystyrenes as a function of average molecular weight between the branch points, $M_s = M_{bb}/(N_{br}+1)$, and molecular weight of the branches, M_{br}: loosely grafted comb (LC), densely grafted comb (DC), loosely grafted bottlebrush (LB), densely grafted bottlebrush (DB). The lines are based on equations 6 to 9. The

scatter plot represents the position of each comb on the diagram according to their M_{br} and their calculated M_s. Values used for calculation: Polystyrene, M_0 = 104.15 g·mol^{-1}, M_e = 14500 g·mol^{-1}, ρ = 0.909 g cm^{-3}, ν = 0.19 nm^3, l = 0.19 nm, b = 1.8 nm.

In **Figure 3**, the comb polymers **5a** to **5d** are placed in the graph according to their M_{br} and M_s values calculated based on equations 6 to 9. As expected, the 'grafting onto' process, used to synthetize the comb polymers, limits the topology of the resulting polymers to loosely and densely grafted combs and, thus, cannot afford any brushes.[14] The better control of the length of the backbone and branches that provides the 'grafting onto' process allow us to reach well-defined branched polymers, essential criteria for our study, albeit limiting the topologies obtained to comb only.

Thermal Treatment of the Comb Polymers

Extrusion is typically conducted at elevated temperature and high pressure (e.g. 250 °C and 300 bar), thus the oxygen content is substantially reduced. Therefore, as a first insight, we investigated the thermal stability of comb polymers bearing triazole ligation points under inert atmosphere (N_2) at 150 °C in order to determine the effect of the topology of the combs, the length of their side chains as well as their weight average molecular weight on the thermal stability of the comb polymers.

Prior to thermally treating the polymer combs, the stability of the TEMPO end group of the backbone (Scheme S1) was assessed. SEC and HR ESI MS analysis (Figures S26-27) reveal that at 150 °C, under inert atmosphere and in the solid state, the polymer undergoes no detectable change up to 22 h. Indeed, the SEC traces (Figures S27) remain unchanged before and after thermal

treatment and the MS peaks (Figures S28) are in excellent agreement with the structure of the initial TEMPO-PS, indicating that no polymer-polymer coupling takes place.

Comparing the response towards temperature and shearing of the loosely-grafted **5a** and the densely-grafted **5b** combs is of high interest to determine the impact of the topology on the stability of the combs. It has to be noted that both comb polymers are based on the same backbone (**2a**) and branches (**4a**) and exhibit a different N_{br}.

The comb polymers **5a** and **5c** exhibit similar N_{br} with 5 and 4 branches, respectively. Both are based on the same backbone **2b**, the comb polymer **5a** features 5 branches **4a** (M_w=3.3 kg mol^{-1}) per backbone and polymer **5c** has 4 branches **4b** (M_w=18.1 kg·mol^{-1}). By comparing the thermal stability of **5a** and **5c**, we establish the effect of the length of the side chain on the stability of the triazole ligation point for LC and DC architectures. In a previous study on photo-generated Diels-Alder cycloadducts located at the mid-chain of a linear polymer, we found a decreasing thermal stability of the ligation point with an increase of the chain length on either side of the connection.[51] Thus, we expect an impact of the length of the branches on the thermal stability of the comb polymers.

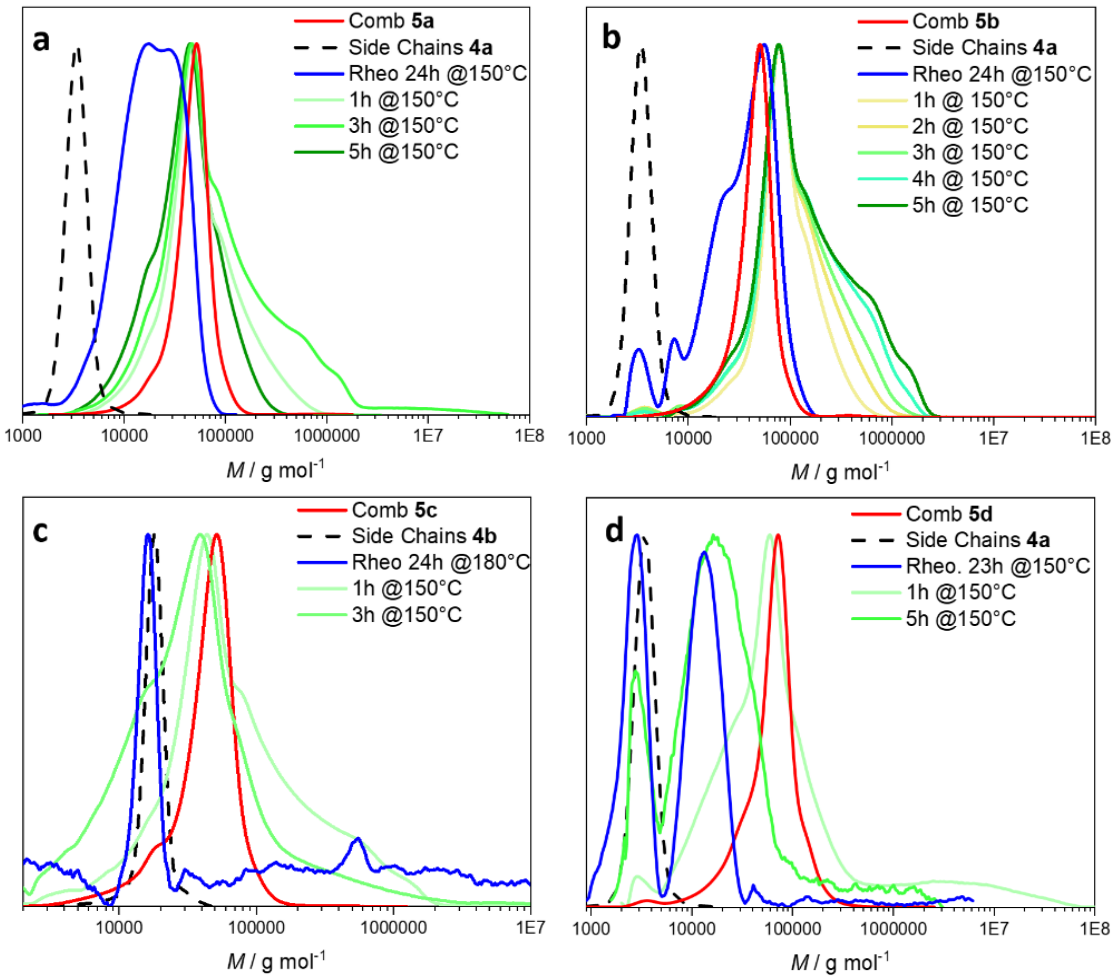

Figure 4. SEC traces of the samples resulting from the thermal degradation of **5a** : PS-40k-5-3.3k LC (**a**), **5b :** PS-40k-39-3.3k DC (**b**), **5c** : PS-40k-4-18k DC (**c**) and **5d** : PS-55k-12-3.3k LC (**d**) for 1 to 8 h at 150 °C under N_2 atmosphere as well as the rheology sample after thermal and shearing treatment at 150 °C or 180 °C and 23 h or 24 h (see the legend) (in THF and with RI detector calibrated using linear poly(styrene) standards ranging from 476 to 2.5 × 10^6 g·mol^{-1}). Blue traces: The rheology sample (refer to the rheology section) were dissolved in THF (a.t. 72 h), filtered and analysed via SEC. The curves are normalized to the highest peak.

Once dried overnight under high vacuum, the comb polymers were placed into tightly closed vials (2 mg per vial and one vial per data point), under nitrogen at 150 °C for 1 to 24 h and

analysed via SEC (RI detection). The SEC traces of the thermally challenged comb polymers **5a**, **5b**, **5c** and **5d** are depicted in

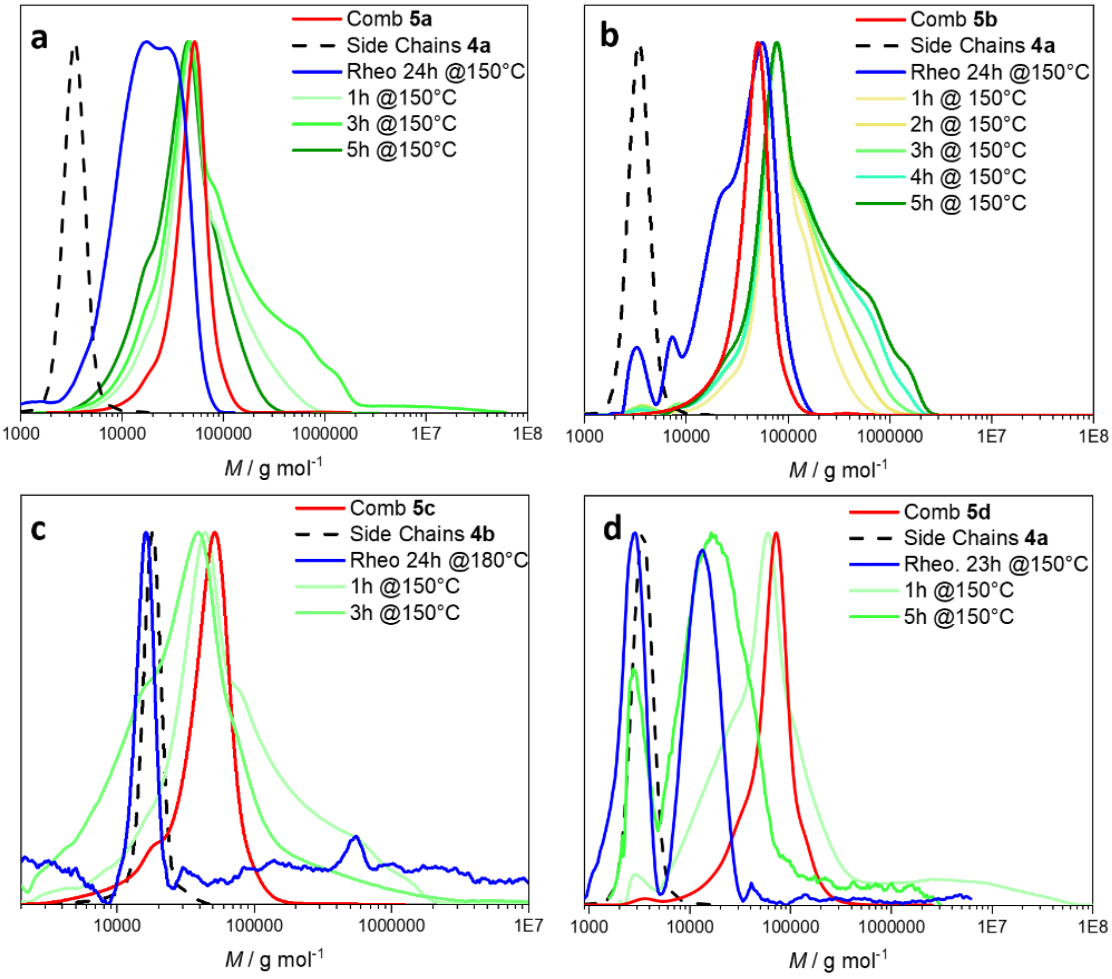

Figure 4. In the SEC traces of the comb polymer **5a**, we observe the appearance of a shoulder at high molecular weight (0.7 to 1.0 10^6 g·mol^{-1}) after 1 h. This observation is likely due to intermolecular bonding occurring between end-chains of the branches. Indeed, the vinyl groups might form radicals that lead to coupling of the combs via their side chains. Altintas *et al.* showed in their study on the thermal stability of triazole moieties in linear polymers a similar behavior, attributed to the formation of acidic HBr in the presence of Br terminated polymers.[43] In the current study, the elimination of HBr occurred during the deprotection of the side chains

thus forming a double bond at the chain termini. Therefore, we assume that the double bonds at the end of the branches are responsible for the intermolecular reactions. After 5 h, the shoulder at high molecular weight decreases, the main trace is shifted to lower M values (~10^4-10^6 g·mol^{-1}). We suggest that the high molecular weight crosslinked material is removed during the filtration prior to SEC analysis. It has to be highlighted that no cleaved side chains **4a** (M_w=3.3 kg·mol^{-1}) are observed by SEC, which is due to either the absence of cleavage of the ligation points or the concentration of cleaved branches being below the detection limit of the SEC's RI detector. Further SEC-HR ESI MS analysis did not allow to visualize the side chains, which may imply that no debonding occurred after 5 h during the thermal treatment of the comb polymer **5a**. In order to ensure that the branches are potentially be detectable if cleaved off the polymer backbone, a mixture of the backbone **2a** and branches **4a** was prepared with the same backbone/side chains ratio as in the comb **5a** (1 eq. backbone **2a** vs. 5 eq. side chains **4a**) and analyzed via MALLS-SEC. The obtained SEC trace is depicted in **Figure S25** and shows that the concentration of branches is far above the detection limit and, thus, we can confirm that no

cleavage of the branches in the comb **5a** at 150 °C up to 5 h (

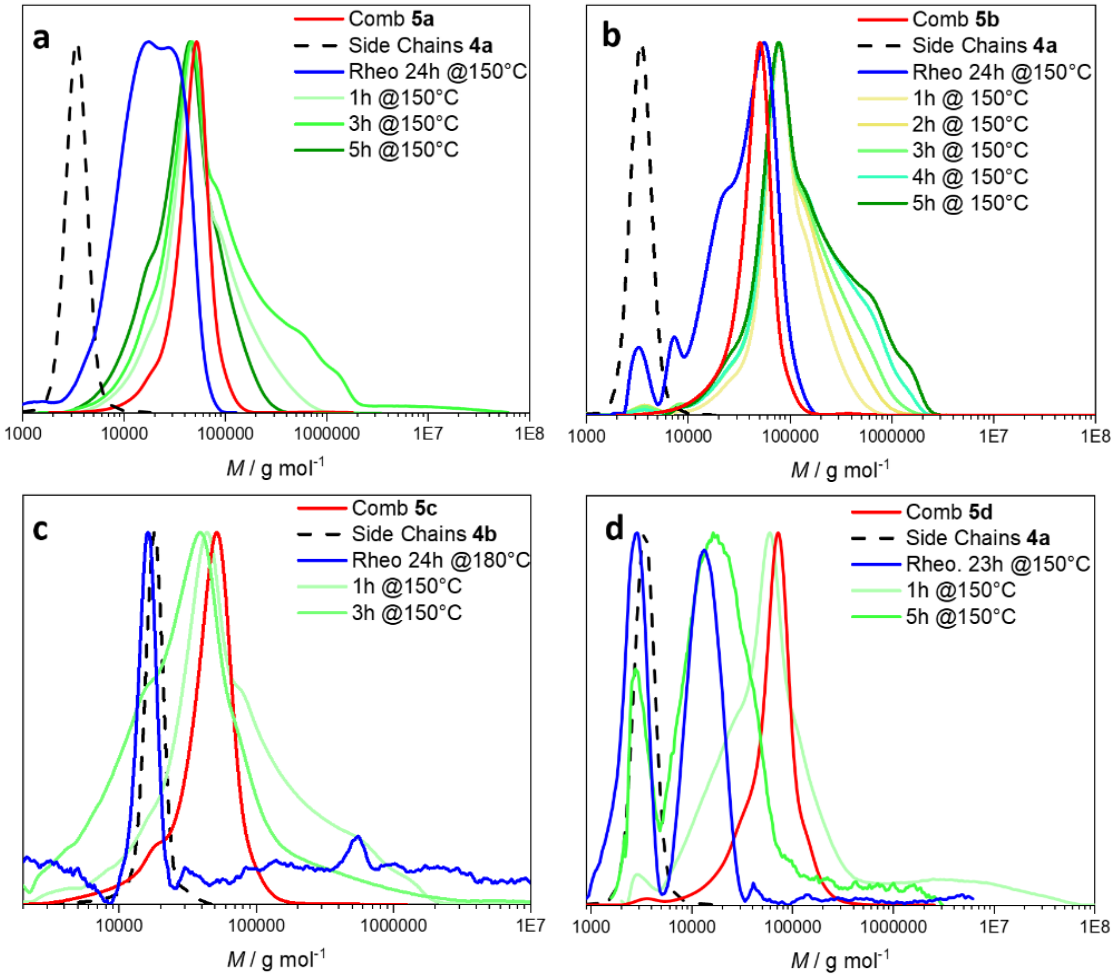

Figure 4a) occurs. In addition, the SEC analysis of the dissolved rheology sample after rheological treatment (**Figure 5-a** blue line) reveal no cleaved branches at low molecular weights (3 kg mol^{-1}) either.

The thermal treatment of comb polymer **5b** was performed in the same fashion as the one for comb **5a**, e.g. at 150 °C under N_2 atmosphere, up to 5-24 h. The resulting SEC trace of each sample is displayed in **Figure 5-a** (the complete time-dependent SEC trace evaluations are available in the Supporting Information **Figure S23**), reveal the appearance of a shoulder at high molecular weight (0.7 to 1.0 10^6 g·mol^{-1}) during the first 5 h of thermal treatment. Here again, we conclude that

intermolecular bonding is occurring and its extent is correlated to the number of branches. Indeed, in comb polymer **5b** there are 8 times more branches than in the comb **5a** (39 branches in **5b** against 5 branches in **5a**) leading to a more pronounced inter-comb coupling phenomenon (intermolecular coupling). In addition, the densely grafted comb **5b** led to gel formation, visible after thermal treatment, which is insoluble in THF. Clearly, there is no material at higher molecular weight values (>10^5 g·mol^{-1}) visible in the SEC trace of the sample after rheological measurement for 24 h at 150 °C (for details refer to the rheology section below). It is therefore very likely that all crosslinked material is included in the gel previously cited and filtered off before SEC analysis.

Contrary to the observations made with the comb **5a**, in **5b** a peak at around 3 000 g·mol^{-1} is detected in the SEC analysis, indicating that the comb polymer degrades at 150 °C. The emerging peak around 3 000 g·mol^{-1} is attributed to the cleaved side chains **4a** (M_w = 3.3 kg·mol^{-1}) along the backbone, while the main peak (~10^4-10^6 g·mol^{-1}) is attributed to the degraded comb polymer. From the SEC analysis – clearly suggesting that the chain length of the degraded fractions (M_w = 3000 g·mol^{-1}) aligns perfectly with the length of the branches – we conclude that the cleavage of side chains occurs during the thermal treatment at the ligation point and an in-depth molecular analysis is required to establish stability of the triazole group. Therefore, SEC-HR ESI MS experiments on the thermally treated comb polymer **5b** were carried out. Since the ESI-MS instrument is limited to 6 000 *m/z* units and since this technique emphasizes the abundance of shorter macromolecules (more likely to be ionized), we focused our study on the cleaved and thermally challenged side chains (3 000 g·mol^{-1}). The mass spectra obtained are displayed in **Figure 5** and the complete time dependent degradation data are available in **Figure S24**. The mass spectra of the thermally treated samples after 1, 5 and 8 h are very similar to each other and exhibit a series of peaks attributed to polystyrene (104 *m*/*z*) with different end groups resulting from the

cleavage of the side chains from the comb polymers. The assignment of the structures presented in **Figure 5** confirms the cleavage of the polymer following two mechanistic routes: (i) opening of the triazole ring with a subsequent cleavage of the C-N bond in the ring and (ii) cleavage of the bond between the carbon atom in para position of the styrene ring and the nitrogen atom of the triazole ring. In addition, the presence of species at 16 mass units higher (in **Figure 5** m/z② = m/z①+16) is attributed to the oxidation of the double bonds at the side chain termini, as has already been observed in a previous study.[51]

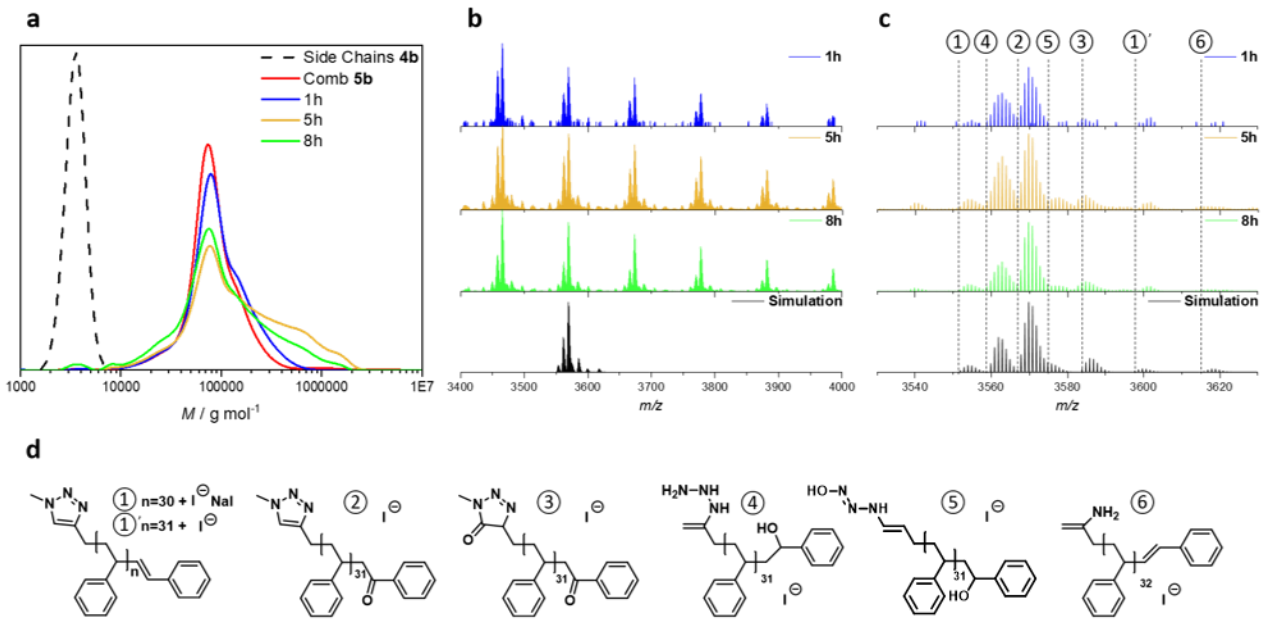

Figure 5. a) SEC traces of the side chains **4b**, the comb polymer **5b** and the degraded comb polymers **5b** after 1 to 8 h at 150 °C under N_2 atmosphere (in THF and with RI detector calibrated using linear poly(styrene) standards ranging from 476 to 2.5 × 10^6 g·mol^{-1}). All peaks are normalized to the total peak area. **b)** SEC-HR ESI MS spectra and **c)** Zoom into one repeat unit of the soluble fractions resulting from the degradation of **5b** after 1, 5 and 8 h at 150 °C under N_2 atmosphere (in THF and with RI detector calibrated using linear poly(styrene) standards ranging from 476 to 2.5 × 10^6 g·mol^{-1}). and **d)** their assigned structures (refer the Supporting Information **Table S1** for the exact values and to the **Figure S28** for the proposed cleavage processes).

In the next step, the combs **5c** and **5d** were thermally challenged using the same process as the previous samples **5a** and **5b**, i.e. dry polymer placed under nitrogen at 150 °C from 1 to 5 h. Both exhibit similar behavior towards thermal treatment resulting, i.e. (i) an increasing shoulder at high molecular weights (up to 10^7 and 10^8 g·mol^{-1} for **5c** and **5d** respectively) attributed to the intermolecular coupling detailed above and (ii) the cleavage of the branches (**4b**: 18.1 kg·mol^{-1} and **4a**: 3.3 kg·mol^{-1} for **5c** and **5d** respectively). While an in-depth molecular study via SEC-HR

ESI MS allowed to highlight the presence of cleaved side chains (M_w=3.3 kg·mol^{-1}) for the comb **5d**, the degraded branches from **5c** have a molecular weight that is too high (M_w=18.1 kg·mol^{-1}) to be visible via this analytical technique.

In summary, we conclude that there is a direct correlation between topology and thermal stability since if any degradation occurs, a loosely grafted comb (LC) would degrade slower than a densely grafted comb (DC). In their study addressing linear polymers containing triazole moieties, Altintas *et al.* concluded that the triazole linkage was thermally stable.[43] A linear system can be considered as a loosely grafted polymer comb in which the pervaded volume of the branches do not overlap and, thus, according to our findings, be stable during thermal treatment.

In addition, the stability of a ligation in a loosely grafted comb agrees with the pervaded volume theory. Indeed, if the spherical volume occupied by each side chain (i.e. pervaded volume of each side chain) comprises side chains from the same comb polymer, the physical forces induced lead to cleavage. In the comb **5c**, for instance, there are 4 side chains having a molecular weight of 18 kg mol^{-1} and a backbone of 40 kg mol^{-1}, implying that the pervaded volume of each chain interpenetrates the one of its next neighbor.

Rheology

Importantly, the thermal stability of the comb polymers was monitored as a function of time via rheological measurements. Small amplitude oscillatory shear (SAOS) experiment in the form of time sweep test was performed on the samples at constant frequency, strain amplitude and temperature under nitrogen atmosphere. The low frequency f = 0.05 Hz ensures sufficient sensitivity to the topological evolutions in comb polymers with time, e.g. side chain cleavage, or

reactions between the double bonds at the end of side chains. Storage modulus, $G'(t)$, loss modulus, $G''(t)$, and absolute value of complex shear viscosity, $|\eta^*(t)|$, were monitored as a function of time. Y_{left}-axis of **Figure 6** shows the evolution of rheological properties of sample **5b** (PS40-39-3.3) by time at 150 °C, under a frequency $f = 0.05$ Hz and a strain amplitude of $\gamma_0 = 0.25$. The same graphs for the samples **5a**, **5c** and **5d** are depicted in the **Figure S22**. Increasing of modulus and viscosity shows that molecular weight is increasing with time, in agreement with the thermal analysis of samples in oil bath in the Y_{right}-axis of **Figure 6**. It was already shown in

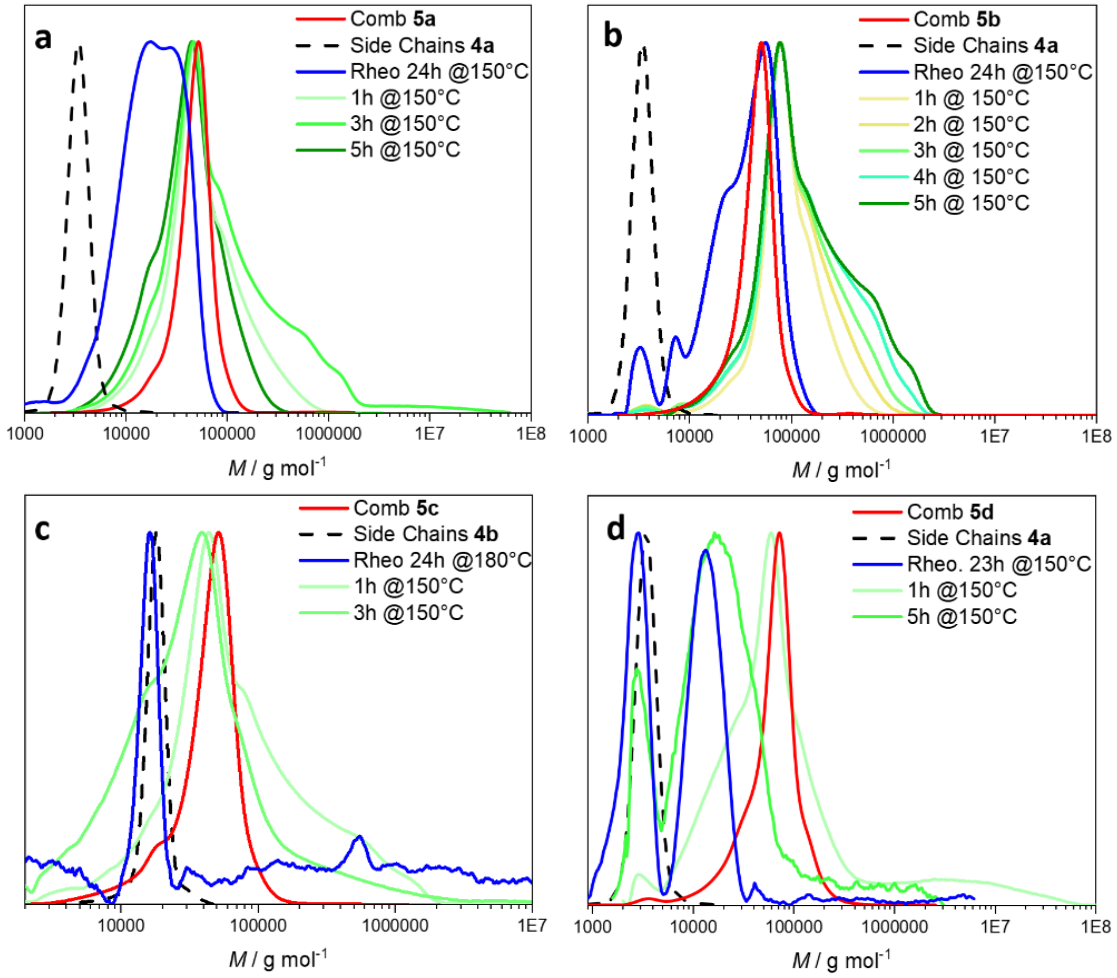

Figure 4b that both cleavage processes of side chains and intermolecular reaction of double bonds at the end of side chains occurred during the thermal process. From a rheological point of view,

the cleavage of the side chains should reduce the zero shear viscosity due to the strong dilution (solvent) effects of detached side chains[52], $\eta_0 \approx \tau G_N^0 \propto M_w^4 \phi_{bb}^4$ according to literature. However, the intermolecular reaction of double bonds strongly increases the molecular weight, M_w, and increases the shear viscosity simultaneously. This reaction is very likely due to the tight spacing between the side chains (double bonds). The rheological experiments displayed in **Figure 6** show that after a thermal treatment of 6 h at 150 °C, the storage modulus crosses the loss modulus, from whereon the polymer behaves like a gel. The SEC data on the Y_{right}-axis of **Figure 6** suggest an artificial reduction in the molecular weight, which is related to filtration of gel contents before injection to the SEC column. It the other words, the rheological data are related to the bulk of polymer including gel contents, while SEC data show only the soluble part of the samples. The rheological data associated with the combs **5a**, **5c** and **5d** are displayed in **Figure S22**.

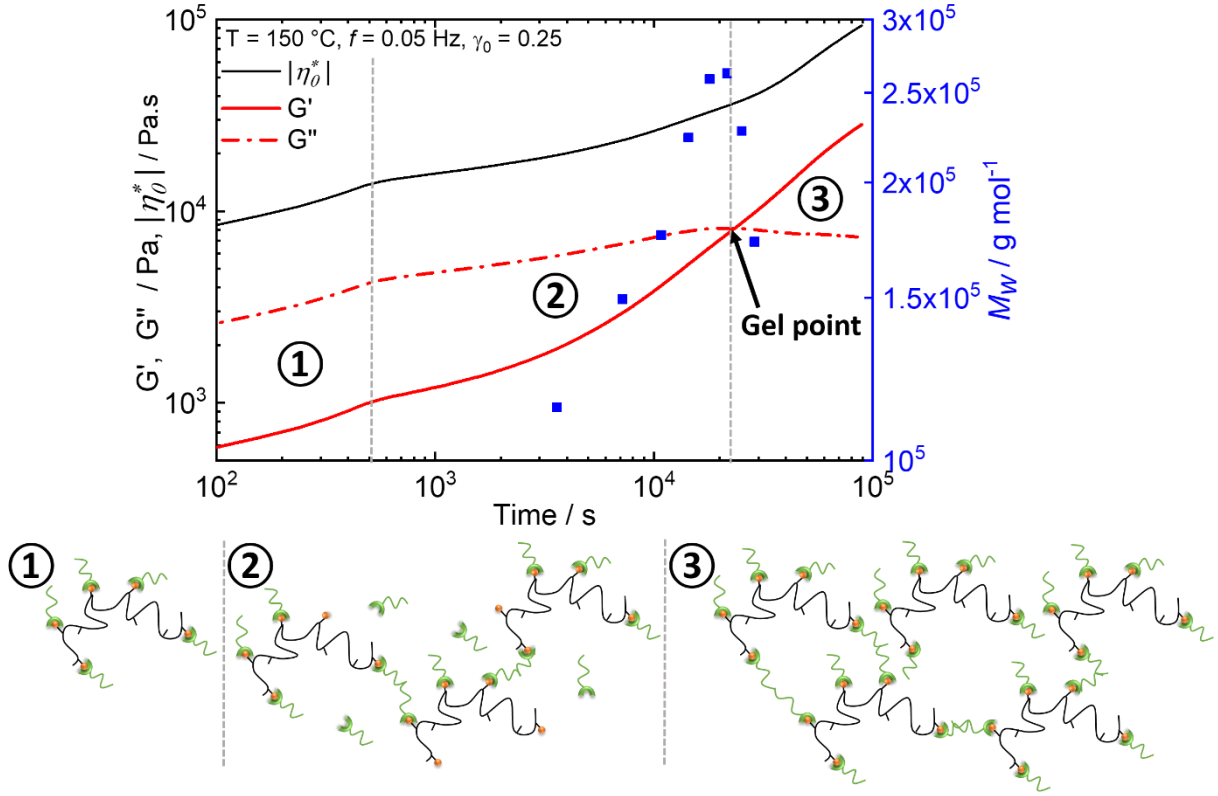

Figure 6. Rheological properties (left axis) of **5b** as investigated with a time sweep experiment at a frequency of 0.05 Hz, a strain amplitude of 0.25 and a constant temperature of 150 °C. Weight average molecular weight (right axis) of samples under thermal treatment in an oil bath measured by SEC. The sections①,②,③ represent the conformation of the sample during rheological testing. With ① being the polymer comb with no modification; ② a mixture of polymer comb, crosslinked system and "free" branches and ③, the gel formed via intermolecular crosslinking.

The rheology sample of the **5b** was dissolved in THF and analyzed via SEC-HR ESI MS; the resulting spectra are displayed in the **Figure 7**.

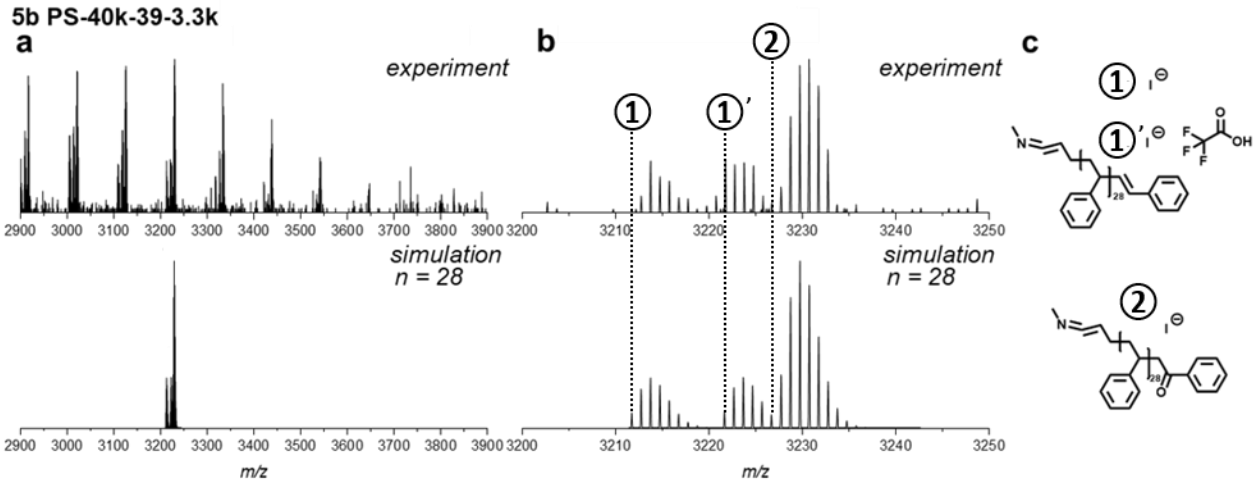

Figure 7. a) SEC-HR ESI MS spectra of the comb polymer **5b** after rheological study for 24 h at 150°C under N_2 atmosphere (in THF). **b)** Zoom on one repetitive unit of the soluble fractions and **c)** Their assigned structures: ①, cleaved branch with I^- ion, ①', cleaved branch with I^- ion and acide trifluoroacetate (hydroxide doping agent) and ②, the oxidized cleaved branch (①+16 *m/z*) with I^- ion (see Supporting Information **Table S2** for the exact values).

The assigned structures resulting from the degradation of the comb polymer **5b** via temperature and shearing at 150°C under inert atmosphere reveal a different process of cleavage than those obtained after thermal treatment only (**Figure 5**). We assume that due to the shearing, the bond between the carbon atom in *para*-position of the ring and the nitrogen atom of the triazole ring cleaves, followed by an elimination of nitrogen and finally a rearrangement of the electrons. The proposed process is depicted in **Figure 8**.

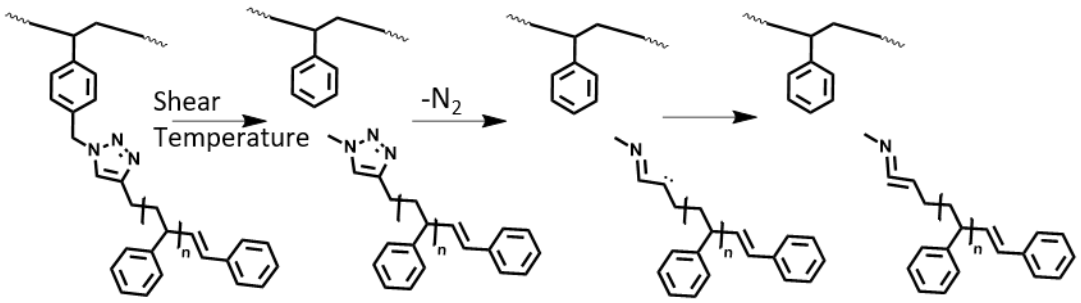

Figure 8. Proposed cleavage process of the branches in the comb **5b** undergoing rheological treatment.

The comb **5b** (PS-40k-39-3.3k DC) is densely grafted, meaning – by definition – that the pervaded volume of its side chains interpenetrates within the same molecule (intramolecular) as well as between different molecules (intermolecular) (**Scheme 3.** Schematic representation of the pervaded volume (grey circle) in the polymer combs **5a** to **5d** with the backbones displayed in black and the branches in green (refer to Table 1 for more details about the combs)-c). The

cleavage of the branches is thus driven by its characteristic topology (

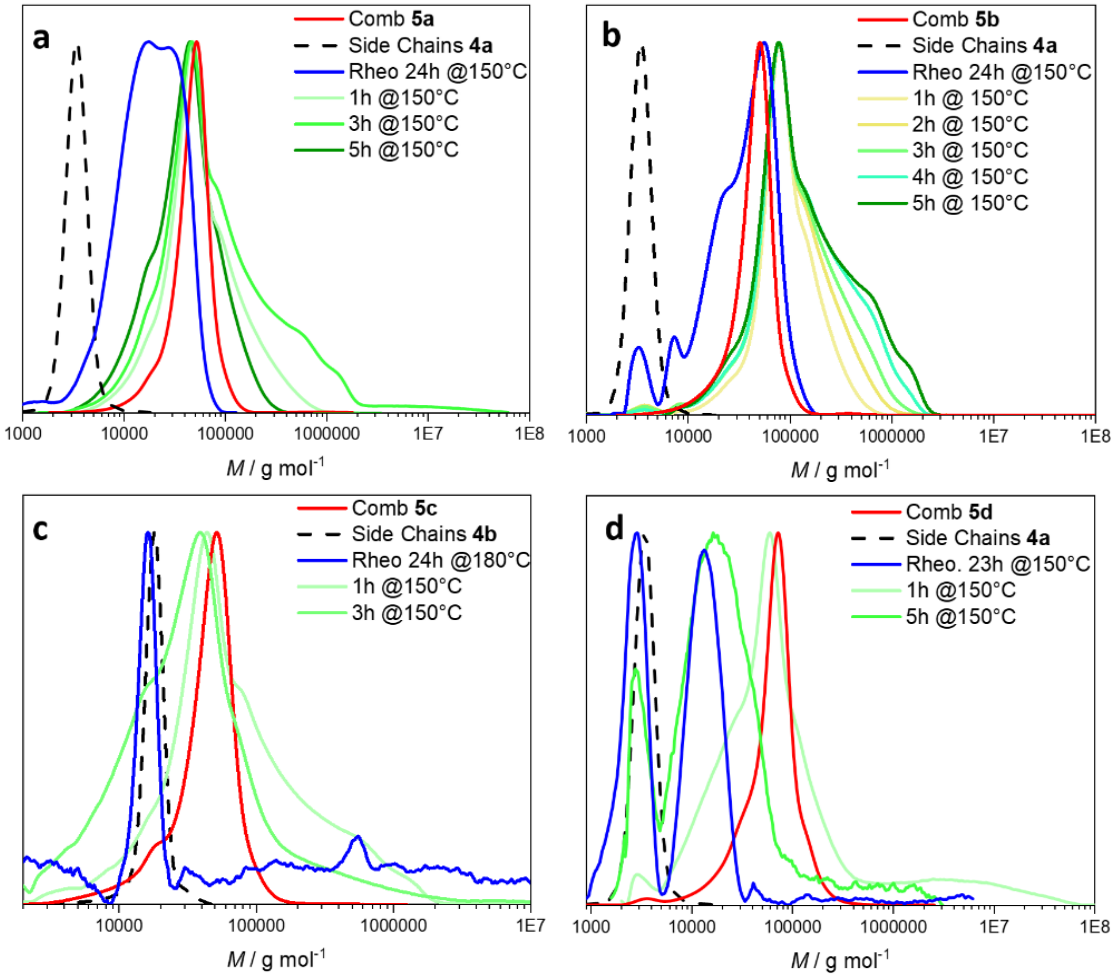

Figure 4-b) as it differs from the LC architecture having similar ligations.

The molecular weight between two branches, M_s, in the polymer comb **5a** (PS-40k-5-3.3k LC) is 6700 g mol^{-1} (**Table 1**) being twice the length of its branches (**Figure 2**), implying that the pervaded volume of the side chains do not interpenetrate each other (**Scheme 3.** Schematic representation of the pervaded volume (grey circle) in the polymer combs **5a** to **5d** with the backbones displayed in black and the branches in green (refer to Table 1 for more details about the combs)-a) neither within one molecule nor between different polymer combs. Consequently,

no cleavage occurs during thermal treatment or rheological study of the polymer comb **5a** (

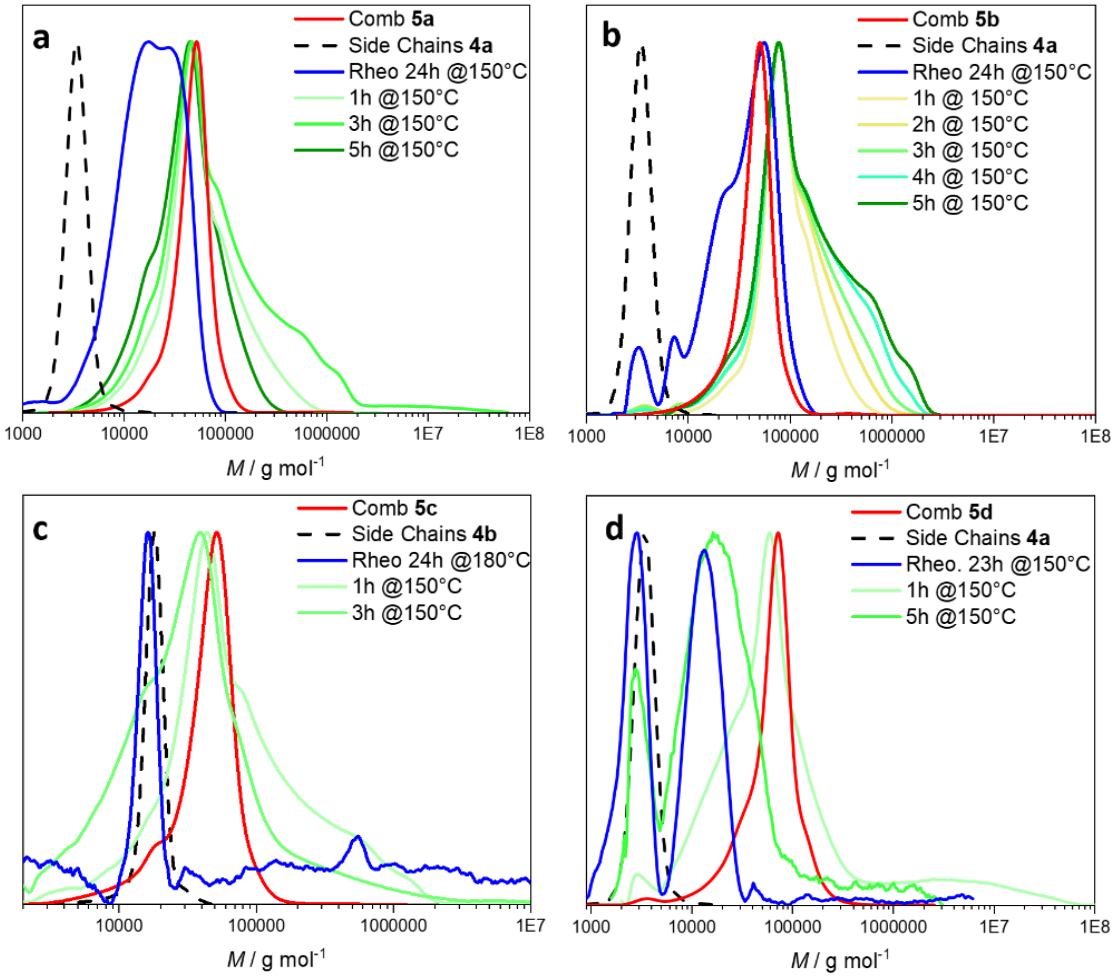

Figure 4-a). As a comparison, in the comb **5c** (PS-40k-4-18k DC), having a comparable number of branches as **5a** (5 and 4 branches per backbone in **5a** and **5c** respectively), the M_s value is 8000 g mol^{-1} (**Table 1**) and the branches have a chain length of 18 kg mol^{-1}. Thus, the expanded pervaded volume (**Scheme 3.** Schematic representation of the pervaded volume (grey circle) in the polymer combs **5a** to **5d** with the backbones displayed in black and the branches in green (refer to Table 1 for more details about the combs)-d) may interpenetrate a pervaded volume from the same polymer comb or from a neighboring one since the M_w of the branches is more

than twice higher than the M_s value. As a result, we observed cleavage of the side chains (

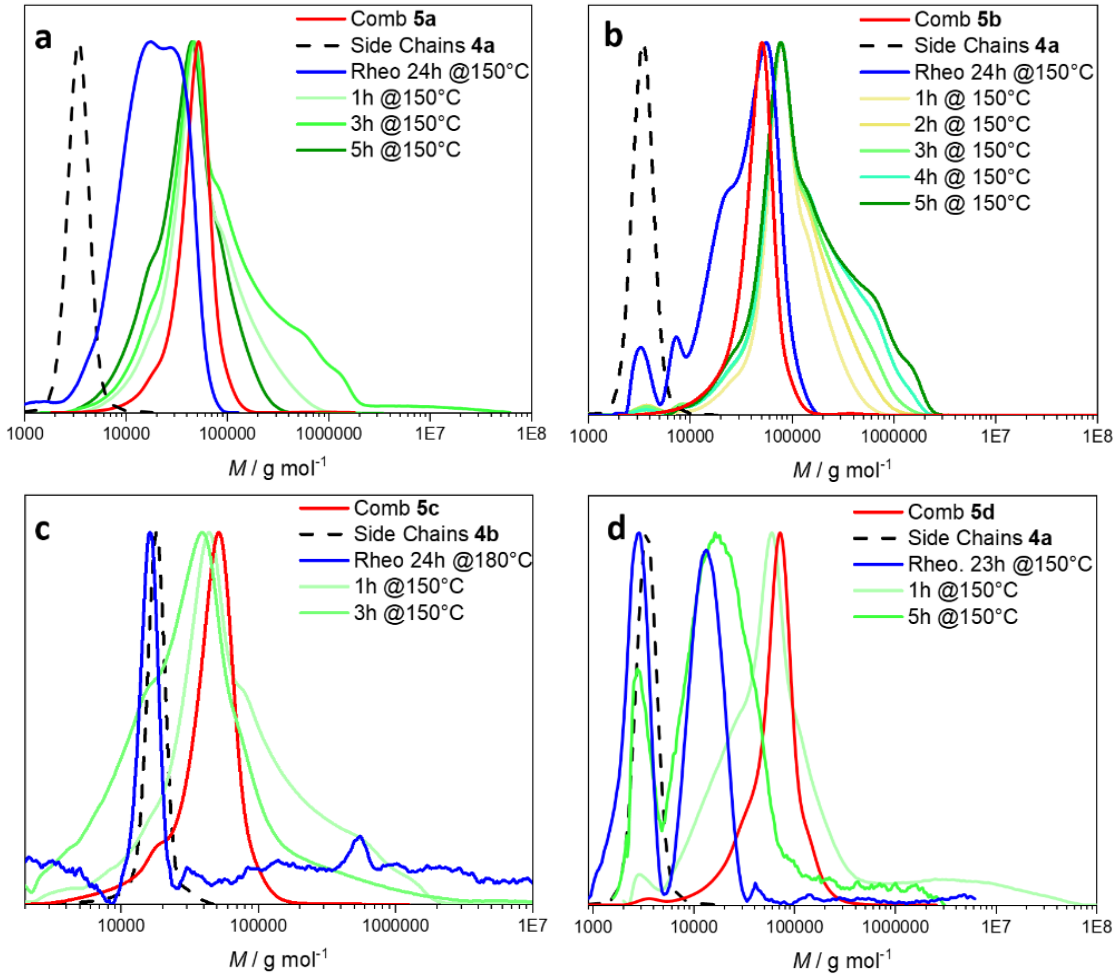

Figure 4-c). When the density of branches increases, yet the comb remains a loosely-grafted topology (as for the comb **5d** (PS-55k-12-3.3k LC)), although its radius is unchanged, the pervaded volume of each side chain is most likely to interpenetrate in an intermolecular or intramolecular manner (**Scheme 3.** Schematic representation of the pervaded volume (grey circle) in the polymer combs **5a** to **5d** with the backbones displayed in black and the branches in green (refer to Table 1 for more details about the combs)**-5d**). As a result, debonding of the branches in the polymer comb **5d –** as experimentally confirmed – occurs.

CONCLUSIONS

We provide a correlation of the molecular architecture of polystyrene (PS) comb homopolymers with their stability to temperature and shear forces on the triazole ligation points joining the branches to the lateral polymer chain. The topology of the comb polymer (both loosely and densely grafted), yet also the number of branches per backbone and the length of the side chains are identified as key parameters for the stability of the triazole ligation point. In a previous study from our group, Altintas *et al.* found that a linear system containing a triazole linkage (in the absence of Br as an end-chain) is stable under thermal treatment and shearing. In the current study, our results highlight the stability of loosely grafted comb up to a limited number of grafted branches. Once the pervaded volume of the branches overlap each other inter- and intramolecularly, the system is no longer stable and the presence of free branches is noticed after thermal and mechanical treatment.

As a result, a densely grafted comb is more likely to degrade than a loosely grafted one and the longer the side chains are, the more readily cleavage occurs. In addition, our study demonstrates that the process of debonding is specific to the type of stress applied to the material. Indeed, when the comb polymers underwent thermal treatment, cleavage occurred under inert atmosphere at 150 °C (or 180 °C), including the formation of intermolecular bonding leading to gel formation. Specifically, the triazole rings cleave by (i) opening of the triazole ring with a subsequent cleavage of the C-N bond in the ring and (ii) cleavage of the bond between the carbon atom in para position of the styrene ring and the nitrogen atom of the triazole ring. In contrast, when shear forces are applied at the same temperatures under inert atmosphere, we observe the cleavage of the bond between the carbon atom in para position of the styrene ring and the nitrogen atom of the triazole ring. However, the elimination of nitrogen results in the formation of a dialkene. We thus submit that the grafting density is a major parameter for controlling the stability of comb polymer

structures constructed by triazole linkages – our findings have thus key implications for such polymers to extrusion processing or molding.

Supporting Information

The Supporting Information is available free of charge on the ACS Publications website at DOI: 10.1021/acs.macromol.xxx. Additional figures, experimental procedures, instrumentation, synthetic procedures, and analysis of the compounds used (PDF).

Corresponding Author

*Email: manfred.wilhelm@kit.edu (M.W.)

*Email: a.goldmann@qut.edu.au (A.S.G.);

*Email: christopher.barnerkowollik@qut.edu.au (C.B.-K.)

ORCID

Charlotte Petit: 0000-0002-8077-6735

Anja S. Goldmann: 0000-0002-1597-2836

Christopher Barner-Kowollik: 0000-0002-6745-0570

Manfred Wilhelm: 0000-0003-2105-6946

Mahdi Abbasi: 0000-0001-6099-421X

ACKNOWLEDGMENTS

C.B.-K. and M. W. gratefully acknowledge financial support from the German Research Council (DFG) for the research projects WI1911/18-2 and BA3751/19-2. C. B.-K. acknowledges the Australian Research Council (ARC) for key funding in the context of a Laureate Fellowship enabling his photochemical research program. The authors thank Dr. Maria Schneider-Baumann (KIT), Dr. Bryan Tuten (QUT) and Lukas Bangert (KIT) for experimental and analytical support.

REFERENCES

(1) Tadmor, Z.; Gogos, C. G., *Principles of polymer processing*. Second Edition ed.; John Wiley & Sons, Inc.: 2006; p 961.

(2) Dealy, J. M.; Read, D. J.; Larson, R. G., *Structure and Rheology of Molten Polymers From Structure to Flow Behavior and Back Again*. Carl Hanser Verlag GmbH & Co. KG: 2018.

(3) Chen, X.; Rahman, M. S.; Lee, H.; Mays, J.; Chang, T.; Larson, R. Combined Synthesis, TGIC Characterization, and Rheological Measurement and Prediction of Symmetric H Polybutadienes and Their Blends with Linear and Star-Shaped Polybutadienes. *Macromolecules* **2011,** 44 (19), 7799-7809

(4) Nielsen, J. K.; Rasmussen, H. K.; Denberg, M.; Almdal, K.; Hassager, O. Nonlinear Branch-Point Dynamics of Multiarm Polystyrene. *Macromolecules* **2006,** 39, 8844-8853

(5) Lee, J. H.; Orfanou, K.; Driva, P.; Iatrou, H.; Hadjichristidis, N.; Lohse, D. J. Linear and Nonlinear Rheology of Dendritic Star Polymers: Experiment. *Macromolecules* **2008,** 41, 9165-9178

(6) Kapnistos, M.; Vlassopoulos, D.; Roovers, J.; Leal, L. G. Linear Rheology of Architecturally Complex Macromolecules: Comb Polymers with Linear Backbones. *Macromolecules* **2005,** 38 (18), 7852-7862

(7) Kempf, M.; Ahirwal, D.; Cziep, M.; Wilhelm, M. Synthesis and Linear and Nonlinear Melt Rheology of Well-Defined Comb Architectures of PS and PpMS with a Low and Controlled Degree of Long-Chain Branching. *Macromolecules* **2013,** 46 (12), 4978-4994

(8) Kempf, M.; Barroso, V. C.; Wilhelm, M. Anionic Synthesis and Rheological Characterization of Poly(p-methylstyrene) Model Comb Architectures with a Defined and Very Low Degree of Long Chain Branching. *Macromol. Rapid Commun.* **2010,** 31 (24), 2140-2145

(9) Lentzakis, H. Pom-pom-like constitutive equations for comb polymers. *Journal of Rheology* **2014,** 58 (6), 1855-1875

(10) Lentzakis, H.; Vlassopoulos, D. Uniaxial extensional rheology of well-characterized comb polymers. *Journal of Rheology* **2013,** 57 (2), 605-625

(11) van Ruymbeke, E.; Orfanou, K.; Kapnistos, M.; Iatrou, H.; Pitsikalis, M.; Hadjichristidis, N.; Lohse, D. J.; Vlassopoulos, D. Entangled Dendritic Polymers and Beyond: Rheology of Symmetric Cayley-Tree Polymers and Macromolecular Self-Assemblies. *Macromolecules* **2007,** 40 (16), 5941-5952

(12) van Ruymbeke, E.; Muliawan, E. B.; Hatzikiriakos, S. G.; Watanabe, T.; Hirao, A.; Vlassopoulos, D. Viscoelasticity and extensional rheology of model Cayley-tree polymers of different generations. *Journal of Rheology* **2010,** 54 (3), 643-662

(13) Zhang, S.; Tezuka, Y.; Zhang, Z.; Li, N.; Zhang, W.; Zhu, X. Recent advances in the construction of cyclic grafted polymers and their potential applications. *Polymer Chemistry* **2018,** 9 (6), 677-686

(14) Hadjichristidis, N.; Pitsikalis, M.; Iatrou, H.; Driva, P.; Chatzichristidi, M.; Sakellariou, G.; Lohse, D., Graft Copolymers. In *Encyclopedia of Polymer Science and Technology*, 2010.

(15) Binder, W. H.; Sachsenhofer, R. 'Click' Chemistry in Polymer and Material Science: An Update. *Macro. Rapid Com.* **2008,** 29, 952-981

(16) Ikeda, T. Glycidyl Triazolyl Polymers: Poly(ethylene glycol) Derivatives Functionalized by Azide–Alkyne Cycloaddition Reaction. *Macromolecular Rapid Communications* **2018,** 39 (8), 1700825

(17) Hutchinson, J. M.; Cortés, P. Physical aging of shape memory polymers based upon epoxy-thiol "click" systems. *Polymer Testing* **2018,** 65, 480-490

(18) Martens, S.; Holloway, J. O.; Du Prez, F. E. Click and Click-Inspired Chemistry for the Design of Sequence-Controlled Polymers. *Macromolecular Rapid Communications* **2017,** 38 (24), 1700469

(19) Barner-Kowollik, C.; Du Prez, F. E.; Espeel, P.; Hawker, C. J.; Junkers, T.; Schlaad, H.; Van Camp, W. "Clicking" Polymers or Just Efficient Linking: What Is the Difference? *Angewandte Chemie International Edition* **2011,** 50 (1), 60-62

(20) Kolb, H. C.; Finn, M. G.; Sharpless, K. B. Click Chemistry: Diverse Chemical Function from a Few Good Reactions. *Angew. Chem. Int. Ed.* **2001,** 40 (11), 2004-2021

(21) Wu, P.; Feldman, A. K.; Nugent, A. K.; Hawker, C. J.; Scheel, A.; Voit, B.; Pyun, J.; Fréchet, J. M. J.; Sharpless, K. B.; Fokin, V. V. Efficiency and Fidelity in a Click-Chemistry Route to Triazole Dendrimers by the Copper(I)-Catalyzed Ligation of Azides and Alkynes. *Angew. Chem. Int. Ed.* **2004,** 43 (30), 3928-3932

(22) Castro, V.; Rodríguez, H.; Albericio, F. CuAAC: An Efficient Click Chemistry Reaction on Solid Phase. *ACS Combinatorial Science* **2016,** 18 (1), 1-14

(23) Yilmaz, G.; Yagci, Y. New photochemical processes for macromolecular syntheses. *Journal of Photopolymer Science and Technology* **2016,** 29 (1), 91-98

(24) Huang, Z. H.; Zhou, Y. Y.; Wang, Z. M.; Li, Y.; Zhang, W.; Zhou, N. C.; Zhang, Z. B.; Zhu, X. L. Recent advances of CuAAC click reaction in building cyclic polymer. *Chinese Journal of Polymer Science (English Edition)* **2017,** 35 (3), 317-341

(25) Perrier, S. 50th Anniversary Perspective: RAFT Polymerization—A User Guide. *Macromolecules* **2017,** 50 (19), 7433-7447

(26) Chiefari, J.; Chong, Y. K.; Ercole, F.; Krstina, J.; Jeffery, J.; Le, T. P. T.; Mayadunne, R. T. A.; Meijs, G. F.; Moad, C. L.; Moad, G.; Rizzardo, E.; Thang, S. H. Living Free-Radical

Polymerization by Reversible Addition−Fragmentation Chain Transfer: The RAFT Process. *Macromolecules* **1998,** 31 (16), 5559-5562

(27) Matyjaszewski, K. Atom Transfer Radical Polymerization (ATRP): Current Status and Future Perspectives. *Macromolecules* **2012,** 45 (10), 4015-4039

(28) Matyjaszewski, K.; Xia, J. Atom Transfer Radical Polymerization. *Chem. Rev.* **2001,** 101 (9), 2921-2990

(29) Ouchi, M.; Terashima, T.; Sawamoto, M. Transition Metal-Catalyzed Living Radical Polymerization: Toward Perfection in Catalysis and Precision Polymer Synthesis. *Chem. Rev.* **2009,** 109 (11), 4963-5050

(30) Kamigaito, M.; Ando, T.; Sawamoto, M. Metal-Catalyzed Living Radical Polymerization. *Chem. Rev.* **2001,** 101 (12), 3689-3746

(31) Moad, G.; Rizzardo, E., The History of Nitroxide-mediated Polymerization. In *Nitroxide Mediated Polymerization: From Fundamentals to Applications in Materials Science*, The Royal Society of Chemistry: 2016; pp 1-44.

(32) Solomon, D. H.; Rizzardo, E.; Cacioli, P. Polymerization process and polymers produced thereby. Patent US4581429, 1986.

(33) Szwarc, M. 'Living' Polymers. *Nature* **1956,** 178, 1168-1169

(34) Jenkins, A. D. Comments on "Living Polymerization: Rationale for Uniform Terminology" by Darling et al. *Journal of Polymer Science Part A: Polymer Chemistry* **2000,** 38 (10), 1729-1730

(35) Klumperman, B., Reversible Deactivation Radical Polymerization. In *Encyclopedia of Polymer Science and Technology*, 2015.

(36) Kurochkin, S. A.; Grachev, V. P. Reversible deactivation radical polymerization of polyfunctional monomers. *Polymer Science Series C* **2015,** 57 (1), 20-31

(37) Gao, H.; Min, K.; Matyjaszewski, K. Synthesis of 3-Arm Star Block Copolymers by Combination of "Core-First" and "Coupling-Onto" Methods Using ATRP and Click Reactions. *Macromolecular Chemistry and Physics* **2007,** 208 (13), 1370-1378

(38) Johnson, J. A.; Finn, M. G.; Koberstein, J. T.; Turro, N. J. Synthesis of Photocleavable Linear Macromonomers by ATRP and Star Macromonomers by a Tandem ATRP−Click Reaction: Precursors to Photodegradable Model Networks. *Macromolecules* **2007,** 40 (10), 3589-3598

(39) Zhang, W.; Xue, M.; Ming, W.; Weng, Y.; Chen, G.; Haddleton, D. M. Regenerable-Catalyst-Aided, Opened to Air and Sunlight-Driven "CuAAC&ATRP" Concurrent Reaction for Sequence-Controlled Copolymer. *Macro. Rapid Com.* **2017,** 38 (22), 1700511

(40) Doran, S.; Yagci, Y. Graft polymer growth using tandem photoinduced photoinitiator-free CuAAC/ATRP. *Polym. Chem.* **2015,** 6 (6), 946-952

(41) Altintas, O.; Riazi, K.; Lee, R.; Lin, C. Y.; Coote, M. L.; Wilhelm, M.; Barner-Kowollik, C. RAFT-based polystyrene and polyacrylate melts under thermal and mechanical stress. *Macromolecules* **2013,** 46 (20), 8079-8091

(42) Wang, Z.; Tao, Y.; Wang, Z.; Yan, J. Synthesis and characterization of poly(N-vinyl-1,2,3-triazole)s derived from monomers obtained by highly efficient Wolff's cyclocondensation. *Polymer Chemistry* **2016,** 7 (18), 3172-3178

(43) Altintas, O.; Josse, T.; Abbasi, M.; De Winter, J.; Trouillet, V.; Gerbaux, P.; Wilhelm, M.; Barner-Kowollik, C. ATRP-based polymers with modular ligation points under thermal and thermomechanical stress. *Polym. Chem.* **2015,** 6 (15), 2854-2868

(44) Offenloch, J. T.; Mutlu, H.; Barner-Kowollik, C. Interrupted CuAAC Ligation: An Efficient Approach to Fluorescence Labeled Three-Armed Mikto Star Polymers. *Macromolecules* **2018,** 51 (7), 2682-2689

(45) Likhtman, A. E.; Ponmurugan, M. Microscopic Definition of Polymer Entanglements. *Macromolecules* **2014,** 47 (4), 1470-1481

(46) Paturej, J.; Sheiko, S. S.; Panyukov, S.; Rubinstein, M. Molecular structure of bottlebrush polymers in melts. *Sci. Adv.* **2016,** 2: e1601478 (11)

(47) Daniel, W. F. M.; Burdyńska, J.; Vatankhah-Varnoosfaderani, M.; Matyjaszewski, K.; Paturej, J.; Rubinstein, M.; Dobrynin, A. V.; Sheiko, S. S. Solvent-free, supersoft and superelastic bottlebrush melts and networks. *Nature Materials* **2016,** 15, 183-189

(48) Kavassalis, T. A.; Noolandi, J. Entanglement scaling in polymer melts and solutions. *Macromolecules* **1989,** 22 (6), 2709-2720

(49) Fetters, L. J.; Lohse, D. J.; García-Franco, C. A.; Brant, P.; Richter, D. Prediction of Melt State Poly(α-olefin) Rheological Properties: The Unsuspected Role of the Average Molecular Weight per Backbone Bond. *Macromolecules* **2002,** 35 (27), 10096-10101

(50) Abbasi, M.; Faust, L.; Riazi, K.; Wilhelm, M. Linear and Extensional Rheology of Model Branched Polystyrenes: From Loosely Grafted Combs to Bottlebrushes. *Macromolecules* **2017,** 50 (15), 5964-5977

(51) Petit, C.; Bangert, L. D.; Abbasi, M.; Wilhelm, M.; Goldmann, A. S.; Barner-Kowollik, C. Stability of Diels-Alder photoadducts in macromolecules. *Polymer Chemistry* **2018**, 9, 3850-3854

(52) Shahid, T.; Huang, Q.; Oosterlinck, F.; Clasen, C.; van Ruymbeke, E. Dynamic dilution exponent in monodisperse entangled polymer solutions. *Soft Matter* **2017,** 13 (1), 269-282

TOC Image

Comb Polymers with Triazole Linkages under Thermal and Mechanical Stress

*Charlotte Petit,[ab] Mahdi Abbasi,[c] Tobias Fischer,[ab] Manfred Wilhelm,[*c] Anja S. Goldmann,[*ab] Christopher Barner-Kowollik[*ab]*